# Green Chemistry

Cutting-edge research for a greener sustainable future

rsc.li/greenchem

TEA

LCA

Hansen
Solubility
Parameters

HIGH
PRESSURE
REACTOR

ROYAL SOCIETY
OF **CHEMISTRY**

**PAPER**
Canan Sener *et al.*
Solvent selection for a biomass-to-bioproduct pipeline
through integrated reductive catalytic fractionation and
microbial funneling

ROYAL SOCIETY OF CHEMISTRY

Check for updates

# Solvent selection for a biomass-to-bioproduct pipeline through integrated reductive catalytic fractionation and microbial funneling

Sarada Sripada, [ID] †[a,b] Juriti Rajbangshi, [ID] †[a,c] Emmanuel A. Aboagye, [ID] †[d] Maximiliano García-Mancilla, [ID] [a,b,e] Timothy J. Donohue, [ID] [a,b,e] Daniel R. Noguera, [ID] [a,b,f] Reid C. Van Lehn, [ID] [a,c] Christos T. Maravelias, [ID] [d] Steven D. Karlen [ID] [a,b] and Canan Sener [ID] *[a,b]

The growing significance of lignin-first biorefineries, which focus on upgrading the aromatics resulting from lignin depolymerization, presents opportunities for bioproduct synthesis using microbial strains capable of funneling a diverse array of phenolics into a single commodity chemical. In this study, we evaluated a biomass-to-bioproduct pipeline involving the reductive catalytic fractionation (RCF) of poplar biomass followed by biological funneling with a *Novosphingobium aromaticivorans* strain that produces 2-pyrone-4,6-dicarboxylic acid (PDC), a potential bioplastic precursor. Considering the impact of solvent on RCF reactor operating pressure, and the potential inhibitory effects of solvent on downstream microbial funneling, we performed an analysis of six pure solvents, namely methanol, ethanol, isopropanol, isobutanol, 1,4-dioxane and ethylene glycol, and different variations of their aqueous mixtures comprising 5 to 50 vol% water. For each pure solvent and solvent/water system, we measured phenolic monomer yields in the RCF process and PDC yields from the phenolic monomers. We then developed correlation models that relate phenolic monomer yields from RCF-derived samples to Hansen solubility parameters to determine solvent descriptors that contribute to high yields. Furthermore, we developed an integrated biorefinery system to estimate the minimum selling price (MSP) of PDC and the associated carbon footprint to identify solvent systems with better costs and sustainability metrics. These analyses resulted in the 50 vol% methanol/water system being identified as optimal because it reduces RCF reactor pressure and is compatible with microbial funneling with *N. aromaticivorans*. This solvent system produced 63 g PDC per kg biomass (264 g PDC per kg lignin) from 85 g phenolic monomers per kg biomass at a reduced reactor pressure of 48 bar (reduced by 26% compared to our previous poplar-to-PDC pipeline). The MSP for this system is $13.98 per kg of purified PDC (carbon footprint of 1.47 kg $CO_2$e per kg), which is about 24% lower than a previously described poplar-to-PDC pipeline and 46% lower than a lignin-to-PDC pipeline that used pure methanol as the solvent. The results from this study illustrate improvements that can be made in lignocellulosic biorefineries that are compatible with the hybrid chemical and biological processes needed to gain value from lignin.

[a]*Great Lakes Bioenergy Research Center, University of Wisconsin-Madison, Madison, WI 53726, USA. E-mail: csener@wisc.edu*
[b]*Wisconsin Energy Institute, University of Wisconsin-Madison, Madison, WI 53726, USA*
[c]*Department of Chemical and Biological Engineering, University of Wisconsin-Madison, Madison, WI 53706, USA*
[d]*Department of Chemical and Biological Engineering, Princeton University, Princeton, NJ, USA*
[e]*Department of Bacteriology, University of Wisconsin-Madison, Madison, WI 53706, USA*
[f]*Department of Civil and Environmental Engineering, University of Wisconsin-Madison, Madison, WI 53706, USA*
†These authors contributed to this work equally.

**Green foundation**

1. This study combines experimental and modeling approaches to identify green and sustainable solvent systems for the reductive catalytic fractionation (RCF) of poplar biomass, with the goal of maximizing the lignin phenolic monomer yields at lower reactor pressures, while minimizing the process economics of the RCF-based biomass-to-bioproduct pipeline.

2. We identified the 50 vol% methanol/water system as optimal because it reduces RCF reactor pressure and is compatible with microbial funneling of the RCF-derived monomers to the bioproduct PDC by *N. aromaticivorans*. The PDC's minimum selling price for the 50 vol% methanol/water system is 24% lower than a pure methanol-based poplar-to-PDC pipeline and has a 28% lower carbon impact score.

3. Future research will focus on expanding the diversity of phenolic monomers that *N. aromaticivorans* funnels into a single bioproduct. The most impactful additions would be the propyl and ethyl side chain products that represent 20–30% of the produced phenolic monomers.

# Introduction

The concerns surrounding the excessive dependence on fossil fuels to fulfill societal needs for fuels, chemicals and materials have propelled a shift towards carbon-neutral technologies.[1,2] Lignocellulosic biomass has emerged as a renewable and cost-effective feedstock to produce value-added fuels, chemicals and materials for industrial applications.[3] Over the last few decades, lignocellulosic biorefining has primarily focused on carbohydrate valorization to produce cellulosic pulp, paper, and biofuels.[4,5] The need to improve the sustainability and economics of lignocellulosic biorefineries has generated an interest in upgrading the lignin fraction of biomass into bioproducts and biofuels.[6] This interest in lignin valorization has led to the emergence of 'lignin-first' biorefineries, which focus on preventing lignin condensation during fractionation of the biomass, often through catalytic depolymerization of the lignin to more stable products. The goal of 'lignin-first' biorefinery designs is to derive greater value (*vs.* burning it as a fuel) from the lignin, while still maintaining efficient valorization of the carbohydrates.[7,8] This strategy enables the use of lignocellulosic

biomass and avoids lignin degradation while enhancing its conversion to biochemicals in downstream processes.[9] In the presence of a metal catalyst and a reductive environment, this process is known as reductive catalytic fractionation (RCF).[4]

RCF is a two-step process that involves initial solvolysis or fractionation of lignin from cellulose and hemicellulose in lignocellulosic biomass at a high temperature (200–250 °C) and pressure (60–100 bar) in an organic solvent,[10] usually a short-chain alcohol like methanol (MeOH) (Fig. S1). The lignin then adsorbs onto the heterogenous catalytic surface and is depolymerized through catalytic hydrogenolysis. Although RCF has largely been performed in MeOH owing to its high delignification efficiency, techno-economic analyses[10–14] have identified the capital cost associated with MeOH's high operating pressure as a significant economic burden on an RCF-based biorefinery. The addition of water as a co-solvent to pure solvents such as MeOH can be advantageous in enhancing the extraction efficiency of lignin from whole biomass and reducing the operating pressure and economic cost.[15] Alcohol/water mixtures have been reported to exhibit higher RCF monomer yields compared to pure solvents (Table 1).[16–18] Due

**Table 1** Current RCF landscape with different solvents under different reaction conditions

| Feedstock | Solvent system | Catalyst | Initial pressure H$_2$ (bar) | Reaction conditions | RCF yield (wt% lignin) | Ref. |
|---|---|---|---|---|---|---|
| NM6 poplar (lignin) | 30 mL MeOH | 0.4 g 5% Pd/C | 30 | 750 mg lignin, lignin/catalyst = 2, $T$ = 200 °C, $t$ = 3 h | 19.9 | 11 |
| Poplar sawdust | 40 mL MeOH | 0.2 g Pd/C | 20 | 2 g biomass, biomass/catalyst = 10, $T$ = 200 °C, $t$ = 3 h | 28.2 | 17 |
| Birch sawdust | 40 mL MeOH | 0.2 g 5% Pd/C | 30 | 2 g biomass, biomass/catalyst = 10, $T$ = 200 °C, $t$ = 3 h | 28.1 | 32 |
| Poplar | 30 mL MeOH | 0.4 g 5% Ru/C | 30 | 2 g biomass, biomass/catalyst = 5, $T$ = 230 °C, $t$ = 4 h | 32.6 | 16 |
| Poplar sawdust | 40 mL EtOH | 0.2 g Pd/C | 20 | 2 g biomass, biomass/catalyst = 10, $T$ = 200 °C, $t$ = 3 h | 19.4 | 17 |
| Poplar | 30 mL EtOH | 0.4 g 5% Ru/C | 30 | 2 g biomass, biomass/catalyst = 5, $T$ = 230 °C, $t$ = 4 h | 27.0 | 16 |
| Birch sawdust | 40 mL EtOH | 0.2 g 5% Pd/C | 30 | 2 g biomass, biomass/catalyst = 10, $T$ = 200 °C, $t$ = 3 h | 17.4 | 32 |
| Birch sawdust | 40 mL IPA | 0.2 g 5% Pd/C | 30 | 2 g biomass, biomass/catalyst = 10, $T$ = 200 °C, $t$ = 3 h | 12.2 | 32 |
| Birch sawdust | 40 mL 1-BuOH | 0.2 g 5% Pd/C | 30 | 2 g biomass, biomass/catalyst = 10, $T$ = 200 °C, $t$ = 3 h | 10.8 | 32 |
| Birch sawdust | 40 mL Diox | 0.2 g 5% Pd/C | 30 | 2 g biomass, biomass/catalyst = 10, $T$ = 200 °C, $t$ = 3 h | 5.1 | 32 |
| Birch sawdust | 40 mL EG | 0.2 g 5% Pd/C | 30 | 2 g biomass, biomass/catalyst = 10, $T$ = 200 °C, $t$ = 3 h | 26.9 | 32 |
| Poplar | 20 mL EG | 0.1 g Pd/C | 30 | 1 g biomass, biomass/catalyst = 10, $T$ = 225 °C, $t$ = 3 h | 20.6 | 34 |
| Poplar sawdust | 40 mL MeOH/water (70/30 v/v) | 0.2 g Pd/C | 20 | 2 g biomass, biomass/catalyst = 10, $T$ = 200 °C, $t$ = 3 h | 44 | 17 |
| Poplar | 30 mL MeOH/water (50/50 v/v) | 0.4 g 5% Ru/C | 30 | 2 g biomass, biomass/catalyst = 5, $T$ = 230 °C, $t$ = 4 h | 33.4 | 16 |
| Poplar sawdust | 40 mL EtOH/water (50/50 v/v) | 0.2 g Pd/C | 20 | 2 g biomass, biomass/catalyst = 10, $T$ = 200 °C, $t$ = 3 h | 43 | 17 |
| Poplar | 30 mL EtOH/water (50/50 v/v) | 0.4 g 5% Ru/C | 30 | 2 g biomass, biomass/catalyst = 5, $T$ = 230 °C, $t$ = 4 h | 32.6 | 16 |
| Eucalyptus sawdust | 40 mL *n*BuOH/water (50/50 v/v) | 0.2 g 5% Pd/C | 30 | 2 g biomass, biomass/catalyst = 10, $T$ = 200 °C, $t$ = 2 h | 50 | 45 |
| Birch sawdust | 40 mL Diox/water (50/50 v/v) | 0.2 g 5% Pt/C | 40 | 2 g biomass, 1 vol% H$_3$PO$_4$, biomass/catalyst = 10, $T$ = 200 °C, $t$ = 4 h | 41.7 | 18 |

to the large number of organic solvents available, solvent screening through experiments alone is physically and economically challenging. This challenge has motivated the use of computational tools to investigate the effect of solvent selection on lignin solubility,[19–22] delignification,[23–27] and biomass conversion,[28] suggesting that similar approaches can be extended to better understand solvent effects in the RCF process. As a result, we are interested in finding alternative solvent systems that reduce the RCF operating pressure while maintaining high monomer yields. Furthermore, in an integrated lignocellulosic biorefinery, the products of chemical transformations need to be compatible with downstream biological processes. In the case of RCF, any solvent remaining after most of it is recovered for reuse has the potential to affect downstream microbial transformations.[11] Therefore, further extending solvent selection considerations to include the microbial conversion into products is necessary to capture solvent compatibility in an integrated biorefinery.

In a previous study, we developed an integrated approach to produce 2-pyrone-4,6-dicarboxylic acid (PDC) from bioenergy crops through chemical depolymerization of lignin into a mixture of phenolic compounds using hydrogenolysis, with MeOH as the solvent, followed by microbial funneling of the phenolic hydrogenolysis products to PDC using an engineered strain of *Novosphingobium aromaticivorans*.[11] The catalyst, Pd/C, was chosen to ensure compatibility of the produced phenolics with microbial transformation to PDC.[11] Non-noble transition metal catalysts (*e.g.*, Ni, Mo, and Co) display higher selectivity for monomers with propyl side chains over those with propanol side chains and using such a catalyst would produce a larger fraction of monomers that would not be microbially converted to PDC.[10,29]

Lignin isolated from poplar biomass gave the highest hydrogenolysis monomer yield (20 wt%, lignin basis) and PDC yield (139.1 g PDC per kg lignin which was 7.52 g PDC per kg biomass).[11] A technoeconomic analysis (TEA) of the integrated poplar-to-PDC biorefinery indicated a PDC minimum selling price (MSP) of $19.70 per kg (2019$, which is equivalent to $25.90 per kg in 2024$) with MeOH as the solvent.[11] Replacing the serial lignin isolation and hydrogenolysis steps with RCF increased the monomer yield (24 wt%, lignin basis) and PDC yield (58.5 g PDC per kg biomass). The TEA of the RCF-to-PDC biorefinery in that study[30] indicated a reduced PDC MSP of $18.39 per kg (2024$), with thick reactor walls to accommodate the 65 bar operating pressure.

In this study, we investigated solvent selection for RCF using an integrated approach that included RCF and microbial funneling experiments to determine yields, computational modeling to assess predictors of phenolic monomer yields for solvent systems, TEA to assess the cost of an integrated poplar-to-PDC biorefinery, and life cycle assessment (LCA) to assess the carbon footprint of the integrated system. We investigated different solvent systems including MeOH, ethanol (EtOH), isopropanol (IPA), isobutanol (IBA), 1,4-dioxane (Diox) and ethylene glycol (EG), and their aqueous mixtures (5–50 vol% water), for a total of 30 solvent systems. We specifically sought

to identify solvent systems that operate under lower pressures, are compatible with microbial funneling by *N. aromaticivorans*, and maximize the RCF monomer and PDC yields. Microbial funneling assays were performed to assess the conversion of the phenolics present in the produced RCF oil with the different solvent systems to PDC with *N. aromaticivorans*. To complement the experimental screening, we developed a computational model to correlate experimentally determined RCF monomer yields and PDC yields with the Hansen solubility parameters (HSPs) of the solvents. We then modeled the operation of an integrated poplar-to-PDC biorefinery for twelve solvent systems (six pure solvents and their respective 50 vol% solvent/water), providing comprehensive TEA and LCA insights into solvent selection and its impact on the integrated lignin-first biorefinery. A schematic depiction of our integrated experimental-modeling approach to optimize solvent selection for the biomass-to-PDC pipeline is presented in Fig. 1.

## Results and discussion

### Effect of solvent on RCF

RCF has been investigated with different solvents including EtOH,[16] IPA,[31] *n*-butanol (*n*BuOH),[32] Diox,[33] and tetrahydrofuran (TFA).[32] In addition, high-boiling point polyols such as EG and glycerol are also gaining significance as RCF solvents[34] (Table 1).

To specifically investigate reaction pressure and phenolic yields as a function of solvent, we performed RCF of poplar biomass with polar protic solvents such as low-boiling MeOH and EtOH, medium-boiling IPA and IBA, high boiling EG, and the polar aprotic medium-boiling Diox (Fig. 2). With the volatile alcohols (MeOH, EtOH, IPA, and IBA), the reaction pressure ranged between 46–60 bar, whereas Diox allowed operation at a slightly lower pressure of 30 bar and EG had the lowest reaction pressure of 7 bar, corresponding to an 88% pressure reduction compared to pure MeOH ($P$ = 60 bar) (Fig. 2a). The high boiling point (197 °C) and low vapor pressure ($P$ = 1 bar at $T$ = 200 °C) of EG compared to the other solvents used in this study enabled the lower operating pressure (Table S1), in agreement with previous studies that have used EG for RCF of lignocellulosic biomass at low/atmospheric pressure.[34,35]

The yields of phenolic monomers obtained with the different solvents were also evaluated (Fig. 2b). With EG, we obtained the maximum observed RCF phenolic monomer yield of 5.1 wt% on a biomass basis (biomass dry weight) which is equivalent to 21.4 wt% on a lignin basis, using 24 wt% as the lignin content of the poplar biomass, which has been measured for the specific poplar sample that we utilized[11] (Fig. 2b and Table S2, Fig. S2). MeOH and EtOH displayed a similar and slightly lower monomer yield of 4.9 wt% on a biomass basis (20–21 wt% on a lignin basis, Fig. S2 and Table S2). A decrease in yield was observed with an increase in C-atoms in the alkyl chain of the alcohol solvents, with IPA and IBA displaying lower phenolic monomer yields
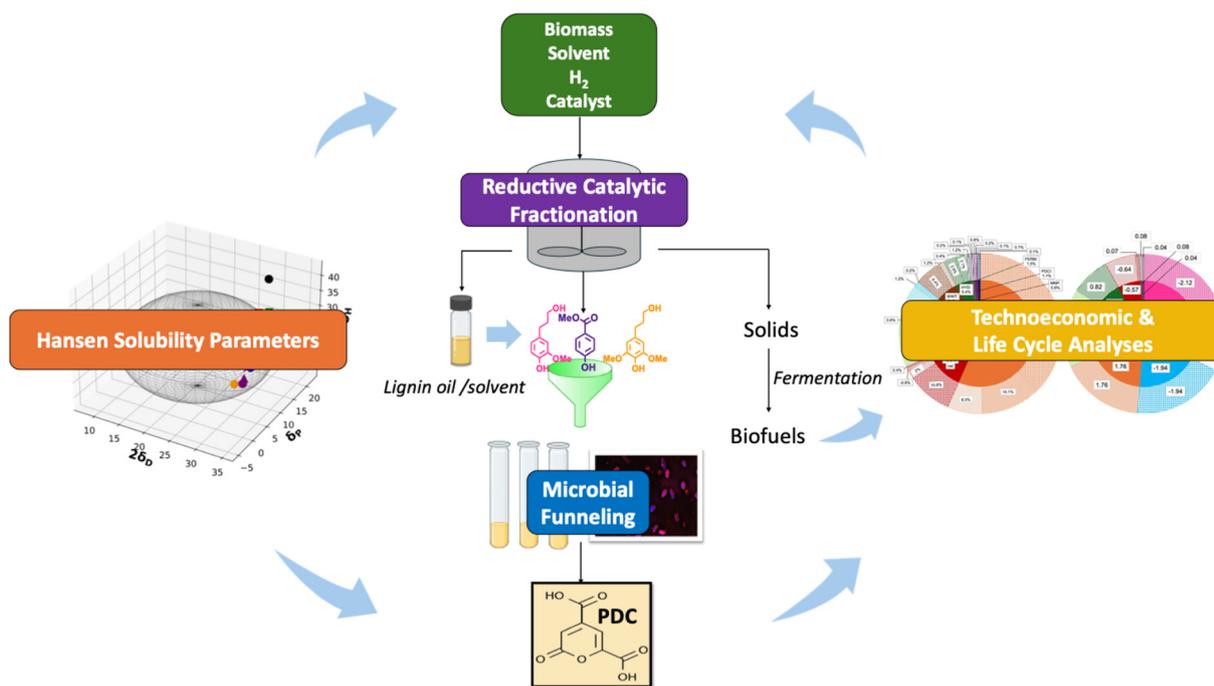
**Fig. 1** Schematic representation of the integrated experimental-modeling approach to optimize solvent selection for the biomass-to-PDC pipeline.
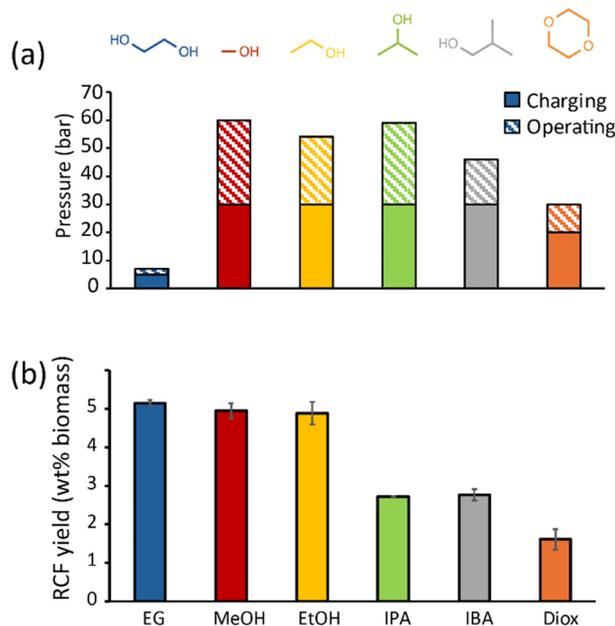


**Fig. 2** (a) Reaction pressure (bar) and (b) RCF monomer yield (wt% biomass) for NM6 poplar with pure solvents of ethylene glycol (EG), methanol (MeOH), ethanol (EtOH), isopropanol (IPA), isobutanol (IBA) and 1,4-dioxane (Diox). Reaction conditions: $T$ = 200 °C, initial pressure = 30 bar (except EG = 5 bar and Diox = 20 bar), $t$ = 2 h, 30 mL solvent, biomass/catalyst = 18. Standard error in panel b was determined from $n$ = 2 technical replicates.

(2.7–2.8 wt% on a biomass basis; 11–12 wt% on a lignin basis) possibly due to reported low lignin dissolution capacity of these alcohols.[36] Diox, a cyclic diether and polar aprotic

solvent that displays high solubility of lignin and lignin-derived phenolics,[37,38] resulted in the lowest observed monomer yield (1.6 wt% on a biomass basis; 6.7 wt% on a lignin basis) compared to the other solvents investigated. This low yield could be due to the solvent competitively adsorbing onto the active sites of the catalyst, limiting access to lignin/phenolic monomers.[39,40] Thus, from a yield perspective, EG, MeOH, and EtOH would be preferred solvents, although EG is the only one of these solvents that allows a reduction in operating pressure (Fig. 2). Since lignin displays both polar (hydroxyl, aldehyde and carbonyl) and non-polar (aromatic rings, ether linkages and methoxy) functional groups,[41] higher lignin solubility and consequently higher RCF yields are expected when using solvents with higher polarity (EG, MeOH, EtOH). These results are also in agreement with reports of EG being a high boiling point solvent that offers high lignin solubility and comparable monomer yields to volatile alcohols such as MeOH and EtOH (Table 1).[42] Facas *et al.*, 2023 reported a yield of 21 wt%, on a lignin basis in the RCF of poplar with EG (225 °C, 3 h, 30 bar $H_2$, Pd/C, biomass/catalyst: 10).[34] Schutyser *et al.*, 2015 reported a slightly higher yield of approximately 27 wt% (200 °C, 3 h, 30 bar $H_2$, Pd/ C, biomass/catalyst: 10).[32]

Since higher RCF yields of phenolic monomers were observed when poplar was treated with EG, MeOH or EtOH, we further investigated the effect of pressure on yield with these solvents. We found that using MeOH and EtOH did not display much variation in monomer yield with pressure. There was a slight increase in phenolic monomer yield (8.5–9.3%) on increasing the pressure from 46 to 70 bar with MeOH, and from 42 to 54 bar with EtOH (Fig. S3). However, we found a 43% increase in monomer yield with EG on increasing the

pressure from 7 to 28 bar. This result indicates that although EG can have a very low operating pressure of 5 bar, the monomer yield is greatly increased when the operating pressure is closer to that of the more volatile organic solvents. This highlights the relationship that reaction pressure has on the amount of dissolved $H_2$, and the critical role that $H_2$ plays in enhancing lignin depolymerization and subsequently the phenolic monomer yield.[31,43]

### Effect of solvent/water mixtures on RCF

The addition of 30–70 vol% water to solvents such as MeOH and EtOH in RCF has been found to confer a synergistic effect, enhancing solvent polarity and thereby improving the extraction of lignin from the biomass, consequently increasing the phenolic monomer yields.[17] However, excess water (>50 vol% with MeOH and >70 vol% with EtOH) has been linked to a reduced degree of delignification and lower monomer yields.[17] To investigate the impact of adding water as a co-solvent on phenolic monomer yields and reaction pressures, we performed RCF reactions in aqueous mixtures of MeOH, EtOH, IPA, IBA, EG, and Diox. Taking into consideration the impact of excess water on monomer yields, as well as issues related to monomer solubility, we investigated RCF with aqueous mixtures of these solvents comprising 5–50 vol% water. Aqueous mixtures of the low and medium boiling alcohols (MeOH, EtOH, and IPA with boiling points of 65, 79, and 82 °C, respectively) resulted in a decrease in the operating pressure by approximately 13–22% compared to the pure solvents when increasing the water content from 5 to 50 vol% in the reaction mixture (Fig. 3a). The addition of water as a co-solvent to these alcohols favors the formation of hydrogen bonds between the solvent and water molecules, enhancing the intermolecular forces between the molecules. These intermolecular forces, as well as the favorable entropy associated with mixing two miscible solvent components, result in an elevation in boiling point and consequent lowering of vapor pressure. Furthermore, the higher the water concentration, the greater the increase in

boiling point (closer to that of water), and the lower the vapor pressure, thereby reducing the reactor operating pressure.[44] In contrast, the measured pressure with the IBA and Diox mixtures remained relatively constant. Aqueous mixtures of EG were operated at 21 bar in the reactor to maintain water in the liquid phase at the reaction temperature (the vapor pressure of water at 200 °C is 15 bar) (Fig. 3a). The reaction pressure with EG/water mixtures ($P$ = 21 bar) was significantly lower (about 65%) compared to pure MeOH ($P$ = 60 bar).

With all solvents, we noted an increase in RCF phenolic monomer yield upon increasing the water content from 5 to 50 vol% (Fig. 3b). The highest RCF phenolic monomer yields were observed with the solvent mixtures comprising 50 vol% water (Table S2, Fig. 3b and Fig. S2). Among the alcohol–water mixtures with 50 vol% water, IPA/water and IBA/water displayed the highest RCF phenolic monomer yield of 9.3–9.4 wt% on a biomass basis, which corresponds to 39 wt% on a lignin basis (Fig. S2). MeOH/water-50 vol% and EtOH/water-50 vol% gave phenolic monomer yields of 8.5 wt% and 8.0 wt%, respectively (35.5 wt% and 33.4 wt% on a lignin basis). Jang and coworkers observed similar RCF monomer yields of 33.4 wt% and 32.6 wt% on a lignin basis with aqueous mixtures of MeOH and EtOH comprising 50 vol% water content.[16] Despite the slightly lower monomer yield of 6.6 wt% with EG/water-50 vol%, the reaction pressure was considerably reduced by about 65% compared to pure MeOH. Upon increasing the water content in the IBA/water mixtures from 5–50 vol% water, phase separation was observed in the reaction mixture and product samples, particularly in the 25 and 50 vol% water mixtures. While studying the RCF of eucalyptus sawdust using a 50 vol% $n$BuOH/water mixture (200 °C, 2 h, 30 bar $H_2$, Ru/C, biomass/catalyst: 10), on cooling the liquor, Renders and co-workers also noted phase-separation.[45]

### Effect of solvent on monomer distribution in RCF oil

RCF of biomass results in an oil containing a mixture of aromatic compounds with different sidechains. The side chain
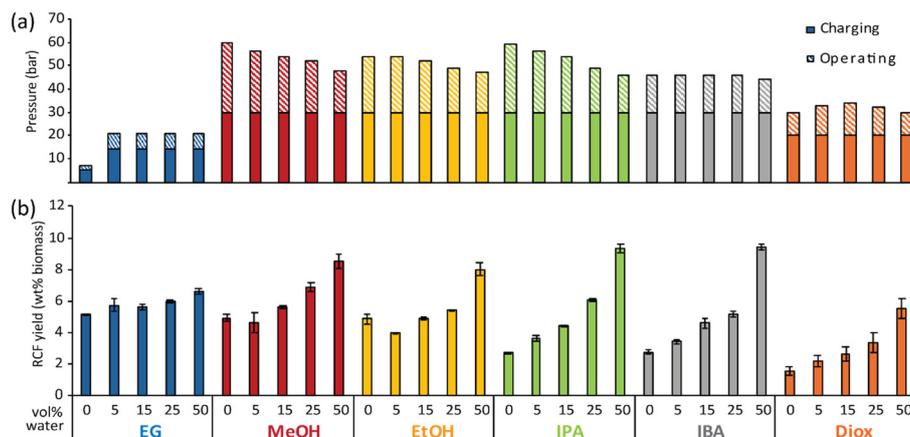


**Fig. 3** (a) Reaction pressure (bar) and (b) RCF monomer yields (wt% biomass) for NM6 poplar with pure solvents and aqueous mixtures (5–50 vol% water). Reaction conditions: $T$ = 200 °C, initial pressure = 30 bar (except EG = 5–15 bar and Diox = 20 bar), $t$ = 2 h, 30 mL solvent, biomass/catalyst = 18. Standard error in panel b was determined from $n$ = 2 technical replicates.

composition of the products depends greatly on the reaction conditions (catalyst and loading, solvent, reaction temperature, residence time and pressure).[11,46] Previous reports using birch and poplar wood with Pd/C as the catalyst showed a high selectivity for propanol side chains 4-(3-hydroxypropyl)-2,6-dimethoxyphenol (S-PrOH) and 4-(3-hydroxypropyl)-2-methoxyphenol (G-PrOH) as the main RCF phenolic products over propane side chains 4-propyl-2,6-dimethoxyphenol (S-Pr) and 4-propyl-2-methoxyphenol (G-Pr).[11,47] Side chain composition is also of importance to achieve compatibility between lignin depolymerization and the downstream biological process that would be used for microbial funneling. Specifically, we have demonstrated that the engineered *N. aromaticivorans* strain used in this study can produce PDC from aromatics comprising propanol, methyl and methyl ester side chains but not from aromatics comprising a propyl, ethyl, or phenol side chain.[11] Furthermore, RCF phenolic products leading to PDC production were identified as S-PrOH, G-PrOH, methyl *p*-hydroxybenzoate (Me-*p*HB), methyl 3-(4-hydroxy-3-methoxy-phenyl)propionate (Me-DHFA), methyl 3-(4-hydroxyphenyl)pro-pionate (Me-DH*p*CA), 4-methylsyringol (S-Me), and 4-methyl-guaiacol (G-Me).[11] Using a Pd/C catalyst, we also demonstrated that with MeOH as the RCF solvent, we could maximize PDC yields by creating a monomer distribution that favored those monomers that the *N. aromaticivorans* strain could transform into PDC.[11]

Thus, we evaluated the monomer distribution and found that changing the solvent system alters this distribution (Fig. 4a and b). The pure solvents displayed high relative levels of S-PrOH and G-PrOH compared to S-Pr and G-Pr. EG displayed the highest proportion of phenolic monomers with pro-panol side chains (88.3% of the quantified monomers) com-pared to the 69–80% present for other solvents (MeOH, EtOH, IPA, IBA, and Diox). The other predominant monomers observed in the RCF phenolic mixture contained propane and ester side chains. Most solvents generated phenolics with propane side chain levels ranging from 9–11%, except for Diox, which displayed products with 18% propane side chains.

The volatile alcohols (MeOH, EtOH, IPA and IBA) displayed ester levels ranging from 13–20%, with the fraction of esters increasing with the number of C atoms in the alkyl chain of the alcohol. The primary ester observed was the *p*-hydroxybenzoate ester of γ-acylated S-PrOH (S-PrO-*p*HB) at concentrations ranging from 13–18 µmol g$^{-1}$ biomass. With MeOH as the RCF solvent, monomers with Me-*p*HB side chains were also observed (11 µmol g$^{-1}$ biomass). In poplar biomass, lignin-bound *p*-hydroxybenzo-ate is released by transesterification to form *p*-hydroxybenzoate esters as one of the major RCF products.[11] EtOH exhibited a similar monomer distribution to MeOH with a low concentration (4 µmol g$^{-1}$ biomass) of ethyl *p*-hydroxybenzoate (Et-*p*HB). Monomers with ester side chains were not detected with EG and Diox, suggesting the possibility of formation of products that were not accounted for in our analysis.

The aqueous mixtures of the solvents displayed varying monomer distribution trends (Fig. 5 and Table S3). Increasing the water content from 5–50 vol% resulted in a decrease in pro-panol proportions with MeOH, EtOH and EG, with this trend more evident in EG. With MeOH and EtOH, increasing the water content in the RCF reaction resulted in a slight decrease in the proportion of phenolic monomers with propanol and ester side chains with a corresponding increase in the pro-panes. With EG, a decrease in the proportion of propanols with a corresponding increase in propanes and esters was observed. However, IPA and IBA displayed different monomer distribution trends than the other solvent water mixtures, with a slight increase in the proportion of propanols and propanes, and with a corresponding decrease in esters. With aqueous mixtures of MeOH, there was an observed increase in the con-centration of the propanol monomers on increasing the water content from 5–50 vol%. In addition, an increase was noted in the concentration of the S-Pr, S-PrO-*p*HB and Me-*p*HB esters. Similar trends were observed with aqueous mixtures of EtOH, IPA, IBA, Diox and EG (Fig. S4 and Table S4). Overall, an increase in the yield of phenolic monomers with propanol, propane, and ester side chains with increase in water content was observed.
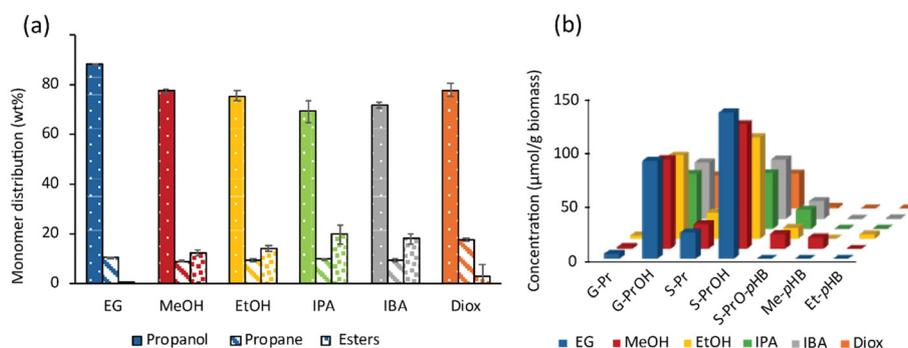


**Fig. 4** Monomer (a) distribution (wt%) and (b) concentration (µmol g$^{-1}$ biomass) for NM6 poplar with pure solvents. Reaction conditions: $T$ = 200 °C, initial pressure = 30 bar (except EG = 5–15 bar and Diox = 20 bar), $t$ = 2 h, 30 mL solvent, biomass/catalyst = 18. Numerical values of the monomer concentrations shown in panel b have been tabulated in Table S4. Standard error in panel a was determined from $n$ = 2 technical replicates.
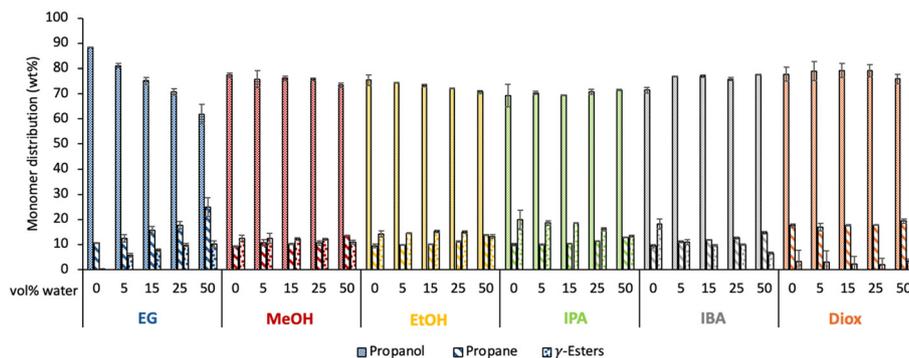
**Fig. 5** Monomer distribution (wt%) for NM6 poplar with pure solvents and aqueous mixtures (5−50 vol% water). Reaction conditions: $T$ = 200 °C, initial pressure = 30 bar (except EG = 5−15 bar and Diox = 20 bar), $t$ = 2 h, 30 mL solvent, biomass/catalyst = 18. Standard error was determined from $n$ = 2 technical replicates.

## Correlation between experimental RCF yield and Hansen solubility parameters

To investigate the observed changes in the phenolic monomer yields across various solvent systems, we examined the correlation between the monomer yields and the Hansen solubility parameters (HSPs)[23,48] of the solvents used in the RCF experiments. We first computed relative energy difference (RED) values (detailed in the SI), which quantify whether lignin should be soluble in each solvent system and have been shown in previous studies to correlate with delignification yields.[23,27,49,50] However, our analysis found that RED values are weakly correlated with RCF monomer yields (Fig. S6), suggesting that the yields are not solely due to increased delignification. We next sought to determine if HSPs can still be suitable descriptors to determine the properties of solvent systems that lead to high RCF yields by parameterizing a multiple linear regression model that relates the three HSPs ($\delta_D$, $\delta_P$ and $\delta_H$) to experimental monomer yields. The best-fit linear regression model is shown in eqn (1), while Fig. S7 shows a parity plot comparing predicted and experimentally determined yields:

$$\text{Yield (wt\%)} = 2.46 - 1.59(\delta_D) - 4.07(\delta_P) + 10.6(\delta_H) \quad (1)$$

Predictions from this linear model achieve an $R^2$ value of 0.84 and RMSE of 0.77 when compared to experimental yields, indicating reasonable model accuracy. Comparison of the regression coefficients shows that $\delta_H$ (the strength of hydrogen bonding interactions) has the largest weight in the linear correlation model, suggesting that solvent systems that maximize this parameter should lead to the highest yields.

To improve the model's accuracy and better represent the complex relationship between the monomer yield and HSPs, we next fitted a quadratic regression model to relate HSPs to experimental monomer yields. The best-fit model is presented in eqn (2) and includes interaction terms consisting of pairwise products of the individual HSPs:

$$\text{Yield (wt\%)} = 14.0(\delta_H) + 1.6(\delta_D{}^2) - 3.9(\delta_P{}^2) - 6.6(\delta_D \times \delta_H)$$
$$(2)$$

Fig. 6 compares the experimental RCF monomer yield (wt% biomass) and the yield calculated using the quadratic regression model. The optimal model has only four parameters and achieves an $R^2$ value of 0.92 and RMSE of 0.56, underscoring the ability of solvent HSPs alone to accurately predict phenolic monomer yields. Comparison of regression coefficients indicates that $\delta_H$ has the largest weight, in agreement with the linear model. This analysis indicates that the solvent systems with higher $\delta_H$ values (50 vol% solvent–water mixtures, as shown in Fig. 3b and Table S2) substantially increase the phenolic monomer yield, which is consistent with the experimental observation that increasing the water content to increase the solvent mixture polarity (higher $\delta_H$ value)
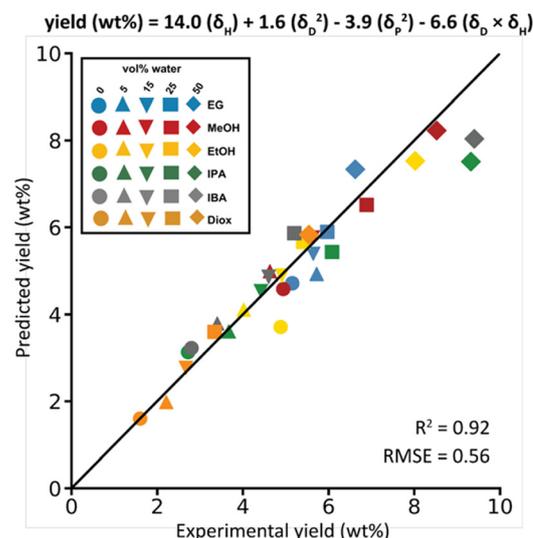


**Fig. 6** Predicted RCF monomer yield (wt% biomass) calculated using a quadratic regression model with interaction terms plotted against the experimental RCF monomer yield (wt% biomass) for pure solvents and their aqueous mixtures (5−50 vol% water) listed in Table S2. The optimized equation for the quadratic regression model with interaction terms (eqn (2)) is also displayed in the figure.

enhances the depolymerization of the lignin oligomers into its monomers,[51] providing a simple design guideline for RCF process improvement.

### PDC yields with different RCF solvents

Microbial funneling experiments with RCF phenolic mixtures were performed to study the impact of RCF solvent selection on RCF monomer to PDC conversion. These experiments diluted (50×) the RCF solvent containing the monomers in defined growth media (SMB) supplemented with glucose (2 g L$^{-1}$). This effectively creates a growth medium that contained 2 vol% of the solvent, simulating that solvent recovery after the RCF process would not be 100% efficient, and therefore, that the microbial funneling process will be exposed to the remaining solvent, albeit with a diluted concentration of the RCF phenolic monomers.[11] This medium was inoculated with the engineered PDC-producing *N. aromaticivorans* strain[11] to evaluate PDC yields. An abiotic control, without inoculation, served to evaluate the potential for non-biological transformation of the phenolic monomers, whereas a positive control containing 1 mM *p*-hydroxybenzoic acid (*p*HBA) was used to evaluate the expected growth and PDC production of the strain when fed a pure aromatic substrate.[52] We found that the engineered *N. aromaticivorans* grew in medium comprising 2 vol% RCF oil derived from five of the pure solvents (EG, MeOH, EtOH, IPA, and Diox) but did not grow in media containing 2 vol% IBA, indicating that IBA was inhibitory at this solvent concentration. To evaluate the inhibitory effect of IBA, we performed growth experiments of *N. aromaticivorans* in the range of 1 to 2 vol% RCF oil in SMB supplemented with glucose (Fig. S9). Since the strain grew in the 1 vol% IBA, this concentration was chosen for subsequent IBA experiments, thus allowing us to evaluate PDC yields without the effect of solvent toxicity (Fig. 7).

A summary of the RCF and PDC yields obtained with the pure solvents is presented in Table 2. Note that we report PDC yields on a biomass basis, which is a comprehensive metric that combines the efficiencies of lignin extraction and depolymerization during RCF with the efficiencies on microbial conversion. With pure solvents (bars denoted with 0 in Fig. 7), the highest PDC yield was 4.6 wt% on a biomass basis (19 wt% on a lignin basis) when MeOH was used as the solvent, followed by 3.5 wt% on a biomass basis (14.8 wt% lignin basis) with EG as the solvent (Fig. 7b and S10). The PDC yields observed with MeOH and EG are correlated with the high RCF phenolic monomer yields (4.9–5.1 wt% biomass basis) obtained with these solvents (Fig. 2b). However, despite showing a similar RCF monomer yield to MeOH and EG, the PDC yield was lower when EtOH was used (2.8 wt% on a biomass basis; 11.8 wt% on a lignin basis). With the other solvents, the observed PDC yield was lower, ranging between 1.4–2.4 wt% on a biomass basis (5.7–10.2 wt% on a lignin basis).

Microbial growth and PDC production by *N. aromaticivorans* were also investigated with RCF oil derived using the solvent/water mixtures (Fig. 7 and Table S2). *N. aromaticivorans* growth was relatively constant across the different mixtures tested,

with the caveat that the experiments with IBA were prepared using a 50% dilution of the RCF oil to eliminate the observed inhibitory effects of IBA (Fig. 7a). For all solvent systems tested, an increase in PDC yield was noted with increased water content in the solvent mixtures, with 50 vol% solvent/water mixtures displaying the highest PDC yields for each solvent. Using 50 vol% solvent/water mixtures with MeOH and IPA gave the highest PDC yields of 6.3–6.4 wt% on a biomass basis (26–27 wt% lignin basis), Table 3. With lignin oils derived from 50 vol% solvent/water mixtures of EG, EtOH and Diox, PDC yields of 4.9–5.9 wt% biomass basis (20.6–24.7 wt% lignin basis) were observed. IBA–water mixture displayed a much lower PDC yield, with the 50 vol% mixture resulting in a PDC yield of 2.3 wt% on a biomass basis (9.7 wt% on a lignin basis). The PDC yields increasing with the increased water content in the MeOH and IPA solvent mixtures is consistent with the high yield of RCF phenolic aromatics found in the lignin oils derived from these solvent mixtures (8.5–9.3 wt% biomass basis; 35.5–38.8 wt% lignin basis) (Fig. 3b).

In addition, to evaluate the efficiency of the microbial transformation as a single process that converts the phenolics derived from the RCF process, PDC yields can also be calculated on a molar basis from the quantified aromatics (Fig. 7c, with propanol, propane, ester, methyl, ethyl and phenol side chains shown in Tables S3 and S4) as well as from the aromatics that *N. aromaticivorans* is known to funnel to PDC (S-PrOH, G-PrOH, S-PrO-*p*HB, Me-*p*HB, Me-DH*p*CA, Me-DHFA, S-Me, G-Me). With EG, there was an increase in PDC yield from the quantified aromatics with increasing water content in the solvent mixture, corresponding to the increase in total RCF monomer yields found in the RCF oils (Fig. 7c). PDC yields (wt% biomass) using lignin oils derived from MeOH-, EtOH- or IPA-treated biomass increased as the water content increased to 5 and 15 vol%, and then decreased with additional increasing water content (25 and 50 vol%). This decrease in PDC yield occurred despite the aromatic concentration continuing to increase with higher water content in the solvent mixture. The decrease in PDC yield with these alcohol/water mixtures could be due to the decrease in propanol to propane ratio with increase in water content, as observed in the RCF monomer distribution trends (Fig. 5). Use of RCF oil from IBA-treated biomass also displayed a similar decrease in PDC yield from the monomers on the addition of water to the solvent mixture. Use of RCF oil from Diox-treated biomass resulted in relatively constant PDC yields from the quantified aromatics across the mixtures, although the concentrations of phenolic aromatics increased with the addition of water.

Higher PDC yields from the quantified phenolic monomers in RCF oil were observed with MeOH, IPA and Diox as solvents compared to those prepared with the other solvents (Fig. 7c). A PDC molar yield greater than 100% indicates the presence of unidentified compounds that are metabolized by *N. aromaticivorans* that contribute to PDC production. These compounds could be esters, phenolic dimers and other oligomers, as has been proposed before.[11]
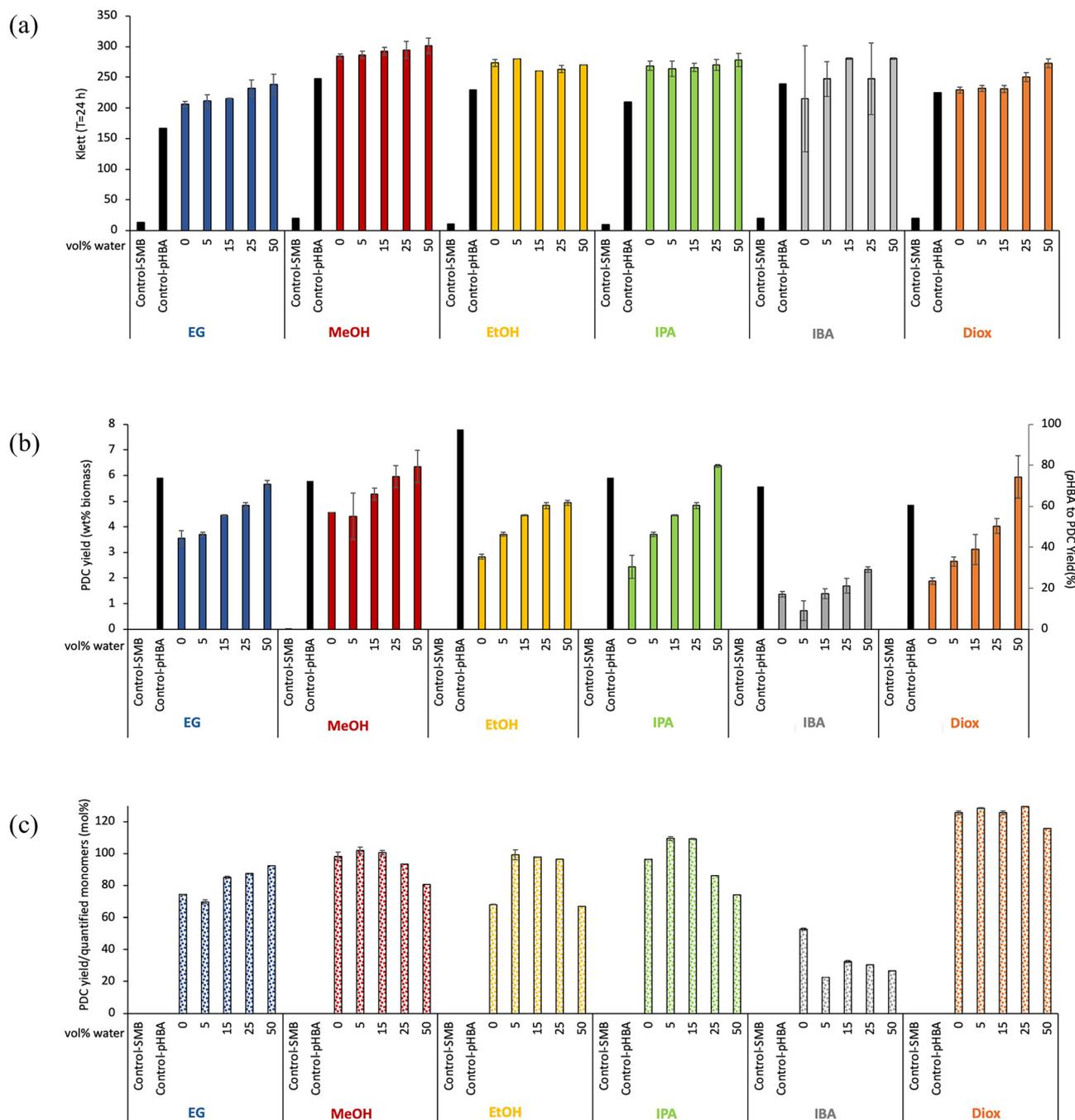
**Fig. 7** (a) Growth, (b) PDC yield (wt% biomass) and (c) PDC yield from quantified monomers (mol%) obtained with *N. aromaticivorans* strain PDC from the RCF aromatics on a biomass basis from pure solvents and aqueous mixtures (5–50 vol%). Culture conditions: SMB media supplemented with glucose (2 g L⁻¹) and 2 vol% RCF oil in solvent (1 vol% for IBA), 24 h, 30 °C, 200 rpm. Standard error was determined from $n = 3$ technical replicates.

**Correlation between experimental PDC yield and HSPs**

Following our analysis of the relationship between solvent HSPs and RCF monomer phenolic yields, we explored whether similar correlations exist between solvent HSPs and the experimental PDC yield obtained from RCF-derived streams. To evaluate this, we developed a quadratic regression model with interaction terms to relate HSPs to experimental PDC yields. The best-fit model is provided in eqn (3) and it includes inter-

action terms consisting of pairwise products of the individual HSPs.

$$\text{Yield (wt\%)} = 14.3(\delta_H) + 2.0(\delta_D{}^2) - 6.3(\delta_D \times \delta_P) - 6.6(\delta_P \times \delta_H) \quad (3)$$

Since the experiments involving IBA were conducted using 1 vol% RCF oil, in contrast to the 2 vol% used for all other

**Table 2** Summary of RCF and PDC yields obtained with pure solvents ethylene glycol (EG), methanol (MeOH), ethanol (EtOH), isopropanol (IPA), isobutanol (IBA) and 1,4-dioxane (Diox)

| | EG | MeOH | EtOH | IPA | IBA | Diox |
|---|---|---|---|---|---|---|
| **RCF yield** | | | | | | |
| g aromatics per kg biomass | 51.5 ± 0.7 | 49.4 ± 2.0 | 48.8 ± 2.9 | 27.2 ± 0.2 | 27.7 ± 1.5 | 16.0 ± 2.7 |
| g aromatics per kg lignin | 214.4 ± 2.8 | 205.9 ± 8.3 | 203.2 ± 12.1 | 113.3 ± 0.7 | 115.4 ± 6.2 | 66.8 ± 11.3 |
| wt% aromatics from biomass | 5.15 ± 0.07 | 4.94 ± 0.20 | 4.88 ± 0.29 | 2.72 ± 0.02 | 2.77 ± 0.15 | 1.60 ± 0.27 |
| wt% aromatics from lignin | 21.4 ± 0.3 | 20.6 ± 0.8 | 20.3 ± 1.2 | 11.3 ± 0.1 | 11.5 ± 0.6 | 6.7 ± 1.1 |
| Total initial monomers for microbial funneling (mM) | 0.24 ± 0.00 | 0.23 ± 0.01 | 0.21 ± 0.04 | 0.13 ± 0.00 | 0.13 ± 0.01 | 0.08 ± 0.01 |
| Convertible initial monomers for microbial funneling (mM) | 0.21 ± 0.00 | 0.21 ± 0.01 | 0.19 ± 0.04 | 0.11 ± 0.00 | 0.11 ± 0.01 | 0.06 ± 0.01 |
| **PDC yield** | | | | | | |
| mM | 0.18 ± 0.02 | 0.23 ± 0.00 | 0.14 ± 0.01 | 0.12 ± 0.02 | 0.07 ± 0.01 | 0.09 ± 0.01 |
| g PDC per kg biomass | 35.5 ± 3.0 | 45.5 ± 0.0 | 28.3 ± 1.0 | 24.4 ± 4.6 | 13.6 ± 1.1 | 18.9 ± 1.3 |
| g PDC per kg lignin | 147.8 ± 12.6 | 189.6 ± 0.0 | 118.0 ± 4.2 | 101.6 ± 19.2 | 56.8 ± 4.4 | 78.8 ± 5.4 |
| wt% PDC from biomass | 3.55 ± 0.30 | 4.55 ± 0.00 | 2.83 ± 0.10 | 2.44 ± 0.46 | 1.36 ± 0.11 | 1.89 ± 0.13 |
| wt% PDC from lignin | 14.8 ± 1.3 | 19.0 ± 0.0 | 11.8 ± 0.4 | 10.2 ± 1.9 | 5.7 ± 0.4 | 7.9 ± 0.5 |
| mol% PDC from quantified aromatics | 74.3 ± 6.3 | 98.3 ± 0.0 | 68.1 ± 2.4 | 96.5 ± 18.2 | 52.9 ± 4.1 | 125.7 ± 8.6 |
| mol% PDC from convertible aromatics | 84.4 ± 7.2 | 109.7 ± 0.0 | 76.4 ± 2.7 | 109.5 ± 20.7 | 59.6 ± 4.6 | 158.1 ± 10.8 |

**Table 3** Summary of RCF and PDC yields obtained with aqueous mixtures (50 vol% water) of the solvents ethylene glycol (EG), methanol (MeOH), ethanol (EtOH), isopropanol (IPA), isobutanol (IBA) and 1,4-dioxane (Diox)

| | EG/water 50 vol% | MeOH/water 50 vol% | EtOH/water 50 vol% | IPA/water 50 vol% | IBA/water 50 vol% | Diox/water 50 vol% |
|---|---|---|---|---|---|---|
| **RCF yield** | | | | | | |
| g aromatics per kg biomass | 66.2 ± 2.0 | 85.2 ± 4.8 | 80.2 ± 4.3 | 93.2 ± 2.7 | 94.0 ± 1.7 | 55.4 ± 5.9 |
| g aromatics per kg lignin | 276.0 ± 8.3 | 355.0 ± 19.9 | 334.1 ± 18.0 | 388.1 ± 11.3 | 391.6 ± 7.0 | 230.8 ± 24.5 |
| wt% aromatics from biomass | 6.62 ± 0.20 | 8.52 ± 0.48 | 8.02 ± 0.43 | 9.32 ± 0.27 | 9.40 ± 0.17 | 5.54 ± 0.59 |
| wt% aromatics from lignin | 27.6 ± 0.8 | 35.5 ± 2.0 | 33.4 ± 1.8 | 38.8 ± 1.1 | 39.2 ± 0.7 | 23.1 ± 2.4 |
| Total initial monomers for microbial funneling (mM) | 0.30 ± 0.01 | 0.39 ± 0.02 | 0.37 ± 0.02 | 0.43 ± 0.01 | 0.43 ± 0.01 | 0.26 ± 0.03 |
| Convertible initial monomers for microbial funneling (mM) | 0.21 ± 0.02 | 0.33 ± 0.02 | 0.31 ± 0.02 | 0.36 ± 0.01 | 0.36 ± 0.01 | 0.20 ± 0.02 |
| **PDC yield** | | | | | | |
| mM | 0.28 ± 0.01 | 0.32 ± 0.03 | 0.25 ± 0.00 | 0.32 ± 0.00 | 0.12 ± 0.01 | 0.30 ± 0.04 |
| g PDC per kg biomass | 56.5 ± 1.5 | 63.5 ± 6.4 | 49.4 ± 0.9 | 63.8 ± 0.5 | 23.3 ± 1.1 | 59.4 ± 8.3 |
| g PDC per kg lignin | 235.2 ± 6.4 | 264.5 ± 26.7 | 206.0 ± 3.9 | 265.7 ± 2.2 | 97.0 ± 4.4 | 247.5 ± 34.4 |
| wt% PDC from biomass | 5.65 ± 0.15 | 6.35 ± 0.64 | 4.94 ± 0.09 | 6.38 ± 0.05 | 2.33 ± 0.11 | 5.94 ± 0.83 |
| wt% PDC from lignin | 23.5 ± 0.6 | 26.4 ± 2.7 | 20.6 ± 0.4 | 26.6 ± 0.2 | 9.7 ± 0.4 | 24.7 ± 3.4 |
| mol% PDC from quantified aromatics | 92.4 ± 2.5 | 80.6 ± 8.1 | 66.8 ± 1.3 | 74.2 ± 0.6 | 26.8 ± 1.2 | 115.7 ± 16.1 |
| mol% PDC from convertible aromatics | 131.6 ± 3.6 | 96.7 ± 9.8 | 80.8 ± 1.5 | 88.7 ± 0.7 | 32.1 ± 1.5 | 146.7 ± 20.4 |

solvent systems due to the observed microbial inhibition at higher concentrations, the IBA data point was excluded from the model for consistency and to avoid bias associated with solvent loading. Fig. 8 compares the experimental PDC yield (wt% biomass) and the yield predicted by the quadratic regression model (eqn (3)). The optimized model, which includes only four parameters, achieves an $R^2$ value of 0.92 and an RMSE of 0.32, highlighting the ability of solvent HSPs to describe solvent systems that lead to high PDC yields. A separate model that includes IBA is presented in Fig. S11. This model exhibits reduced accuracy, with an $R^2$ value of 0.89 and RMSE of 0.52 and seven fitted parameters. Comparison of the regression coefficients in eqn (3) again indicates that $\delta_H$ has the largest weight, consistent with the trend observed in the RCF monomer yield model. This suggests that solvent systems with higher $\delta_H$ values, such as 50 vol% solvent–water mixtures

(Fig. 7b), are associated with increased PDC yields obtained from RCF-derived streams. Since the RCF-derived streams includes both monomers and additional PDC precursors (e.g., oligomers), this model reflects both trends in RCF yields and microbial conversion efficiency without explicitly separating the contributions of these two processes to PDC yields. Consequently, solvents with higher $\delta_H$ values are preferred not only for optimizing the RCF process to achieve higher monomer yield, but also for maximizing PDC production.

### Technoeconomic and life cycle analyses

We also used the results of RCF and microbial funneling experiments to perform a comparative TEA and LCA for systems with pure solvents as well as 50 vol% solvent/water systems. We present the MSP for each system here; the simulated process configurations are shown in Fig. S12–23 and a
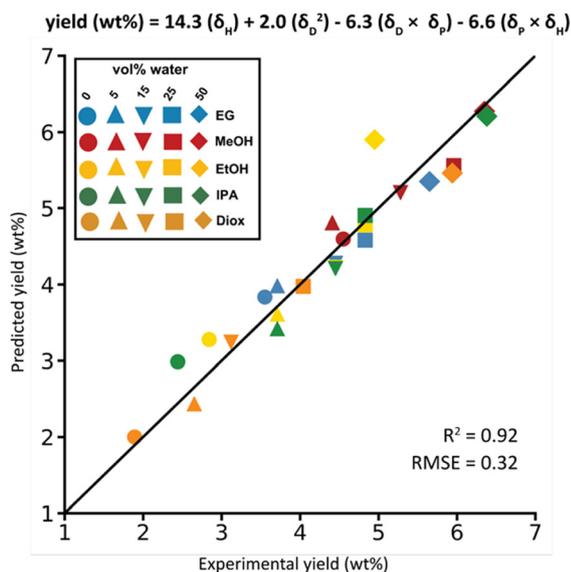
$$\text{yield (wt\%)} = 14.3\,(\delta_H) + 2.0\,(\delta_D^2) - 6.3\,(\delta_D \times \delta_P) - 6.6\,(\delta_P \times \delta_H)$$



**Fig. 8** Predicted PDC yield (wt% biomass) calculated using a quadratic regression model with interaction terms model plotted against the experimental PDC yield (wt% biomass) for pure solvents and their aqueous mixtures (5–50 vol% water) listed in Table S2. The optimized equation for the quadratic regression model with interaction terms (eqn (3)) is also displayed in the figure. Note that the IBA data points are excluded from the model.

detailed breakdown across each block for each system is given in Fig. S24. For the LCA which is based on the carbon footprint (CF) metric, we present the mass allocation results, with that of economic allocation given in Fig. S25. Finally, we perform

sensitivity analysis for the most promising systems to identify opportunities for improving both the MSP and CF.

Fig. 9a shows the MSP, RCF block capital expenses (CAPEX), and the PDC yield for all twelve systems. We observe that systems that have higher PDC yields have lower MSP—MeOH/water ($13.98 per kg), IPA/water ($16.32 per kg), and Diox/water ($14.07 per kg). Furthermore, the solvent/water systems achieve a relatively lower MSP compared to their pure solvent counterparts because in addition to improved PDC yields, they operate at a reduced reactor pressure (except for the EG–EG/water), leading to decreased reactor capital costs. For example, the MeOH system, operating at 60 bar reactor pressure, results in $313 million total reactor costs, while the MeOH/water system at 48 bar achieves a 29% reactor costs reduction.

We observe that the capital recovery charge, which represents the total system CAPEX, is the largest contributor to the MSP, followed by material and fixed costs, respectively; revenue from biofuel and electricity (in some systems) partially offsets these costs. In most systems, the CAPEX contributes between 60–70% to the MSP. In both the EtOH and Diox systems ($58.16 and $90.09 per kg, respectively), we observe substantial material costs mainly due to make-up solvent expenses. Although solvent losses in the Diox system (2.3%) are lower than those in the EtOH system (3.4%), the higher purchase price of dioxane ($2.47 per kg) compared to ethanol ($0.87 per kg) results in considerable expenses. Furthermore, given the high solvent amount in all systems, even small percentage losses translate into significant make-up expenses. The higher material expenditure observed in the IBA/water system stems primarily from the normalization to 1 kg PDC,
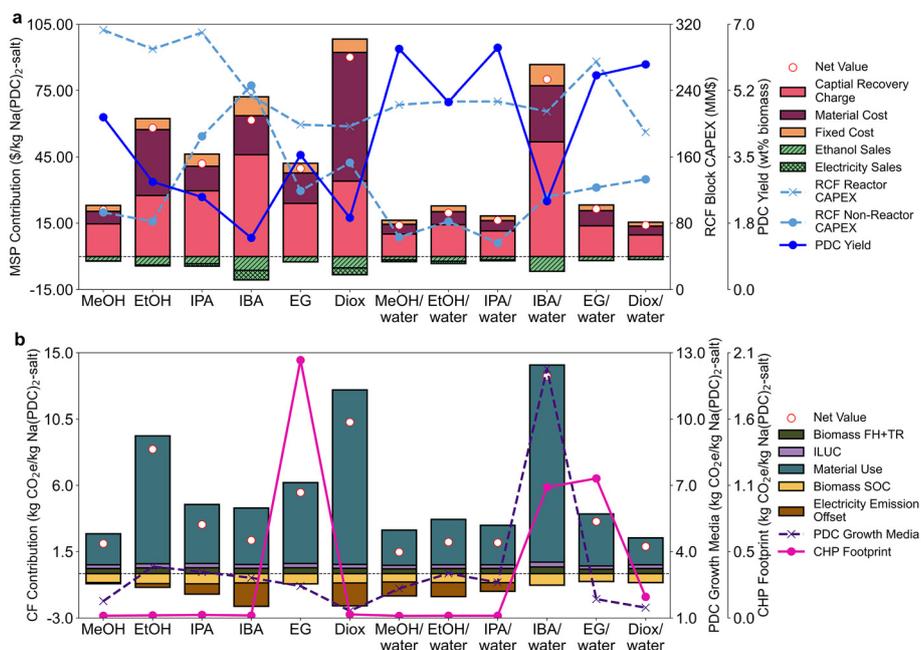


**Fig. 9** MSP (a) and CF (b) of pure solvent and 50 vol% solvent/water systems. Abbreviation: FH: farm handling, TR: transportation, ILUC: induced land use change, SOC: soil organic carbon sequestration, CHP: combined heat and power.

where the lower PDC yield leads to apparent high growth media cost, even though its absolute consumption is comparable to that of the other systems. Additional contribution is due to natural gas purchase to meet heating requirements.

In addition to the higher PDC yields, the systems with lower MSP (MeOH/water, IPA/water, and Diox/water), have other operational advantages. For example, the MeOH/water and IPA/water systems have comparatively lower make-up solvent costs ($0.07 and $0.08 per kg, respectively), and reduced heating and electricity requirements which translate into surplus electricity production, and thereby additional revenue from electricity sales ($0.79 and $0.47 per kg, respectively).

Due to the substantial amount of solvents required for effective biomass fractionation (~21.8 L per kg dry biomass), implementing heat integration strategies within the RCF and monomer purification (MNP) blocks can significantly minimize heat demand. Accordingly, we implement, in all systems, improvements such as (1) flash separation in series, (2) vacuum distillation, and (3) preheating the recovered solvent with the vapor streams from the flash units to reduce heat demand. Without these improvements, all analyzed systems would require natural gas to supplement the heat demand, resulting in a substantial increase in MSP and CF.

Fig. 9b illustrates the CF for all the systems. While material-related emissions emerge as the largest contributor to CF, significant variations are observed. Most emissions are attributed to (1) impacts associated with glucose for PDC growth media production, (2) make-up solvent, (3) natural gas combustion for heat, and (4) grid electricity usage. For example, about 91% (12.3 kg $CO_2$e per kg) of the material impacts for the IBA/water system is attributed to PDC growth media production. However, we observe that the pure solvent systems generally have a higher net CF compared to the solvent–water systems (except for the IBA–IBA/water system). Biomass handling (farming and harvesting) and transportation (ranging between 0.3–0.5 kg $CO_2$e per kg across systems), and induced land-use change (0.2–0.3 kg $CO_2$e per kg) contribute moderately to CF. Biomass soil organic carbon sequestration further offsets some emissions (−0.5 to −0.8 kg $CO_2$e per kg). Systems with surplus electricity generation also benefit from electricity offsets (0.08–1 kg $CO_2$e per kg).

### Sensitivity analyses

To identify opportunities for economic and environmental impact improvements, we performed a single-point sensitivity analysis. Fig. 10 shows the results for the three most promising systems: MeOH/water (Fig. 10a and d), IPA/water (Fig. 10b and e), and Diox/water (Fig. 10c and f). The analysis suggests that fixed capital investment is the major economic driver, with a 50% reduction leading to a 38–40% reduction in MSP across the systems (Fig. 10a–c). Substantial reductions can also be achieved (21% for MeOH/water, 18% for IPA/water, 22% for Diox/water) with reductions in the RCF block CAPEX. Similar
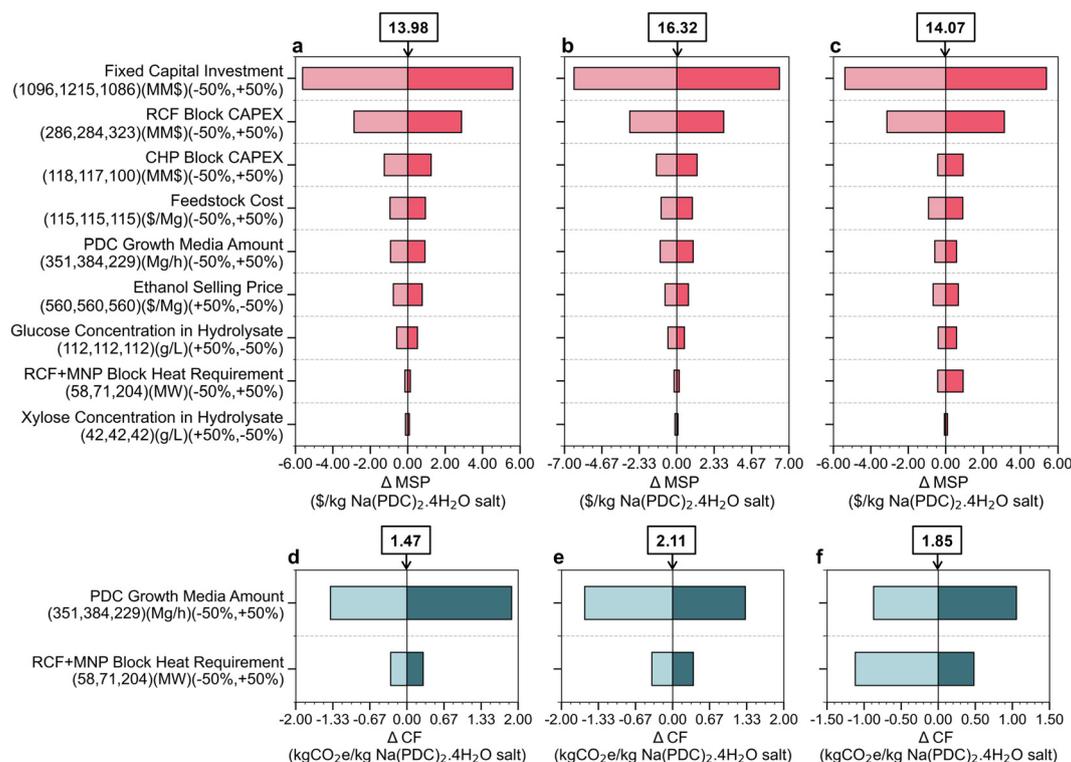


Fig. 10 Sensitivity analysis for the most promising systems. (a) and (d) MeOH/water system, (b) and (e) IPA/water system, and (c) and (f) Diox/water system.

reductions can also be achieved through a decrease in the CHP block CAPEX. Changes in the biomass feedstock and biofuel prices, PDC growth media amount, and glucose concentration have moderate impacts on the MSP. Furthermore, reductions in RCF and MNP block heat requirements have higher impact on the Diox/water system relative to the other two, due to the switch from electricity purchase to selling surplus electricity to the grid. From a sustainability perspective (Fig. 10d–f), it is observed that a reduction in the PDC growth media requirement has the highest impact on the CF for both the MeOH/water (93%) and Diox/water (75%) systems. In the Diox/water system, heat reduction in the RCF and MNP blocks has a higher impact due to offset emissions from surplus electricity.

### Solvent selection for the biomass-to-PDC pipeline

The main goal of this research was to identify solvent systems that could operate at low RCF reactor pressures, display compatibility with *N. aromaticivorans*, and generate high monomer and PDC yields at a lower cost and carbon footprint of an integrated biorefinery system than those in a previous MeOH-based biorefinery design.[30] While MeOH has been extensively investigated as an RCF solvent owing to its high polarity and lignin extraction efficiency, high reactor pressure necessitating the use of thick-walled reactors limit its commercial viability.[10] From an RCF standpoint, 50 vol% solvent/water systems of the alcohols (MeOH, EtOH, IPA, and IBA) achieved higher monomer yields ranging from 8–9.4 wt% (biomass basis) at a reduced reactor pressure of 20–23% compared to pure MeOH.

The 50 vol% IBA/water system generated the highest monomer yield of 9.4 wt% on a biomass basis. This system formed a biphasic reactor product mixture comprising the aromatics in the organic phase when cooled to room temperature. Thus, mixtures of IBA and water as solvents for biomass fractionation could serve as an effective option for the downstream separation of phenolic monomers.[45] Bugli and co-workers performed RCF of poplar sawdust in a 50 vol% of 1-butanol (1-BuOH) and water at an operated reactor pressure of 24 bar, indicating the potential to further lower the reaction pressure for the IBA/water mixture used in this study.[53]

Despite high lignin solubility in aqueous mixtures of Diox (complete lignin dissolution in Diox occurs at a volume fraction of 0.6),[54] the 50 vol% Diox/water system achieved a lower monomer yield, possibly due to the lower $\delta_H$ value compared to the other solvent systems. Moreover, concerns surrounding the formation of peroxides, carcinogenicity and negative environmental impacts likely limit the large-scale industrial applications of Diox as an RCF solvent.[37]

The 50 vol% EG/water system displayed a considerably high RCF monomer yield of 6.6 wt% on a biomass basis (27.6 wt% lignin basis). We observed that the addition of water as a co-solvent in the EG/water system increased the reactor pressure to 21 bar relative to the 7 bar of the pure EG system. However, despite the pressure rise, the EG/water system still operated at a reactor pressure 65% lower than that of the pure MeOH system.

Microbial funneling of the RCF aromatics in the different solvent mixtures also gave higher PDC yields with the 50 vol% solvent/water mixtures than with pure solvents. Equivolumetric aqueous mixtures of MeOH and IPA gave higher PDC yields of 6.3–6.4 wt% on a biomass basis. The RCF reactor pressure with these solvent systems was lowered by 20–22% compared to the pure solvents (46–48 bar). Despite the high monomer yield with an equivolumetric aqueous mixture of IBA, microbial funneling of the RCF aromatics in this solvent mixture with *N. aromaticivorans* resulted in a low PDC yield of 2.3 wt% on a biomass basis. Although a 50 vol% IBA/water mixture is an effective solvent for generating high RCF monomer yields from NM6 poplar, with potential for further reducing the reaction pressure, phase separation, affecting the consumption of aromatics by *N. aromaticivorans*, limits its applications for the biomass to PDC pipeline. 50 vol% aqueous mixtures of Diox and EG also generated high PDC yields (5.6–5.9 wt% on a biomass basis).

Computational correlations between HSPs and the experimental RCF monomer and PDC yields indicate that the 50 vol% solvent/water systems generated higher monomer and PDC yields due to increased hydrogen bonding interactions (associated with higher $\delta_H$ values) that enhance the depolymerization of the lignin oligomers into its monomers.[51] From the TEA and CF perspectives, the 50 vol% MeOH/water ($13.98 per kg), Diox/water ($14.07 per kg), and IPA/water ($16.32 per kg) systems have the lowest MSP, with a corresponding CF of 1.47 kg $CO_2$e per kg, 1.85 kg $CO_2$e per kg, and 2.11 kg $CO_2$e per kg, respectively.

While the TEA and LCA models identify 50 vol% MeOH/water as one potential optimized solvent system for the biomass-to-PDC pipeline, numerous other solvent options, not evaluated in this study, may also be suitable. The proposed workflow for identifying useful solvent systems begins with HSP-based solvent selection, followed by experimental confirmation of the RCF and PDC yields, and concluding with the TEA and LCA modeling. To demonstrate that the regression model developed in this study (eqn (2)) can be used to screen and prioritize promising solvent systems for RCF based on their HSPs, prior to experiments, we performed leave-one-solvent-out cross-validation (detailed in the SI), in which the model was fitted by excluding data for one of the solvents and its aqueous mixtures (*i.e.*, leaving that solvent out during model training), and this was then used to predict yields for the left-out solvent (and its aqueous mixtures). Table S24 summarizes $R^2$ and RMSE values obtained when leaving out each of the solvents while Fig. S26 shows an example parity plot obtained when using EtOH as the left-out solvent. $R^2$ and RMSE values varied from 0.82–0.98 and 0.52–0.89 respectively for all solvents except for EG, thereby achieving comparable model accuracy to the best-fit quadratic regression model. The lower accuracy for EG is because of its high $\delta_H$ value compared to other solvents, which leads to extrapolation during cross-validation that decreases prediction accuracy. A similar approach for the model for PDC yield led to comparable results (Table S25 and Fig. S27).

Overall, these results suggest that the models developed in this study could be used for rapidly screening ranking potential solvent systems for RCF and PDC yields, which can guide experimental validation and solvent optimization. We note that the HSP-based regression models are currently limited to a small set of operating conditions, all at the same temperature. Additional experiments under alternative reaction conditions would be needed to further generalize the models such that trends are transferable across varied reaction conditions. The weaker performance of the models for extrapolation also suggests that the models could be further improved through active learning approaches in which solvent systems are rationally selected for experimental study based on expected model improvement (*e.g.*, by selecting systems that require extrapolation).[55] The TEA model developed in this study can also be integrated with the regression model to further screen potential RCF solvents by considering key economic factors including RCF operating pressure/reactor capital expenses, monomer and PDC yields, energy for solvent recovery, and thereby the MSP of the solvents. This combined strategy has the potential to reduce the number of required experiments. Furthermore, although the models were developed for the production of PDC in this study, they can be adapted for other biomass-to-bioproduct pipelines.

## Conclusions

This study presents both experimental data and a model of a biomass-to-bioproduct pipeline to produce PDC, a bioplastic precursor, through integrated chemical depolymerization and biological funneling. We investigated the use of RCF as a biomass pretreatment method with various pure solvents and their solvent/water systems, aiming to identify systems that could operate at lower reactor pressures, while improving RCF monomer yields. We find that the reactor pressure at 200 °C could be lowered to 21 bar with an EG/water system; however, the lower RCF monomer yield produced under those conditions and the more costly solvent recovery result in a higher MSP. 50 vol% solvent/water systems of IBA, IPA and MeOH generate higher RCF monomer yields. We further carry out microbial PDC production studies to determine the impact of various solvents on PDC production by *N. aromaticivorans*. Despite a high monomer yield with IBA/water 50 vol%, this solvent system is not compatible with *N. aromaticivorans*, and 50 vol% solvent systems of IPA and MeOH produce higher PDC yields. Next, we develop a regression model to relate experimental RCF monomer and PDC yields to Hansen solubility parameters, which quantify dispersive interactions, dipole–dipole interactions, and hydrogen bonding interactions ($\delta_H$). We find that solvent systems with higher $\delta_H$ values significantly increase RCF monomer and PDC yields. Finally, we perform TEA and LCA analyses of twelve systems using an integrated biomass-to-PDC biorefinery approach. We identify 50 vol% MeOH/water as the most economically viable (MSP of $13.98 per kg) system. This system also achieves the lowest CF

(1.47 kg $CO_2$e per kg) and could operate at a lower pressure (48 bar) relative to pure MeOH (60 bar). The outcomes of this study provide a better understanding of the significance of solvent selection for biomass conversion to bioproducts through integrated chemical and biological processes. Furthermore, the regression model can be used as a screening tool for ranking and prioritizing promising solvent systems for RCF and PDC yields. When coupled with experimental validation and TEA and LCA analyses, this approach can expedite solvent screening for biomass-to-PDC pipelines. Future work will focus on extending the current solvent screening framework by incorporating reaction kinetics at multiple temperatures and mechanistic studies such as DFT calculations and spectroscopic monitoring to provide insight into why higher $\delta_H$ values improve monomer and PDC yields. In addition, the development of descriptors that can explicitly capture catalyst–solvent interactions will be further explored to improve the scope of the current screening framework.

## Methods

### Chemicals and materials

The catalyst, Pd/C, and all the solvents used in this study (MeOH, EtOH, EG, IPA, IBA and Diox) were procured from Sigma-Aldrich. NM6 hybrid poplar (*Populus maximowiczii × nigra*) was used for all the experiments and has been described previously. The NM6 hybrid poplar was debarked, chipped, dried, and fractionated to pass through a 5 mm round hole on a shaker table. The poplar biomass was further milled for 30 Hz for 3 min in a shaker mill to obtain a fine powder.[11] PDC was produced by culturing *N. aromaticivorans* 12444Δ*ligI*Δ*desCD* in SISnc-V0 media supplemented with 3 mM *p*HBA and 0.5 g L$^{-1}$ (2.8 mM) glucose, and purified following a simplified version of the published methods,[56] obtaining a >97% pure chemical standard for GC-MS and LC-MS quantification.

### Reductive catalytic fractionation (RCF)

RCF reactions with different solvents (MeOH, EtOH, IPA, IBA, Diox, EG), and their aqueous mixtures (5–50 vol% water) were performed in a 50 mL Hastelloy Parr reactor equipped with a heating mantle and mechanical stirrer (Fig. S28). We did not exceed a water fraction of 50 vol% in the solvent/water mixtures to avoid issues with the solubility of lignin monomers in the solvent. The reaction mix comprised 1377 mg biomass, 77 mg Pd/C (biomass-to-catalyst: 18 : 1 w/w), 30 mL solvent, and 0.21 mg mL$^{-1}$ 1,2-dimethoxybenzene as internal standard for determining the monomer yields. The reactor was sealed and purged with argon (3×) and subsequently purged (3×) and pressurized with hydrogen gas to 30 bar for the volatile alcohols MeOH, EtOH, IPA and IBA, 20 bar for Diox and its aqueous mixtures, 5 bar for EG and 15 bar for its aqueous mixtures. The batch vessel was heated to 200 °C at a ramp rate of 6 °C min$^{-1}$ and held there for 2 h ($T$ = 200 °C, $P$ = 7–60 bar). Post reaction, the heating mantle was removed, and the reactor

was rapidly cooled to room temperature by quenching in a chilled water bath. Once the reactor reached room temperature, it was slowly depressurized (to minimize the loss of volatile product). The catalyst and residual solids were separated from the mixture using a 1 μm PTFE filter. The product mixture (lignin oil in solvent) was stored at 4 °C for further use. RCF oil in solvent obtained from reactions with aqueous mixtures with 75 vol% and 50 vol% IBA were biphasic at room temperature. The mixtures were converted into monophasic solvent mixtures by the addition of MeOH (1 : 3–1 : 6 MeOH : RCF oil/solvent), creating a ternary solvent mixture.

### Microbial strains, growth media and culture conditions

PDC production experiments were carried out with a strain of *N. aromaticivorans* DSM12444 with deletion of the *ligI* and *desCD* genes (strain 12444Δ*ligI*Δ*desCD*).[57,58] Cultures were pre-grown at 30 °C and shaking at 200 rpm in SMB media, which contains 20 mM $Na_2HPO_4$, 20 mM $KH_2PO_4$, 7.5 mM $(NH_4)_2SO_4$, 0.167 mM $ZnSO_4$, 0.125 mM $FeSO_4$, 0.028 mM $MnSO_4$, 0.006 mM $CuSO_4$, 0.009 mM $Co(NO_3)_2$, 0.016 mM $Na_2B_4O_7$, 24.319 mM $MgSO_4$, 1.667 mM $CaCl_2$, and 0.013 mM $(NH_4)_6Mo_7O_{24}$. For routine microbial culture and storage, the SMB media was supplemented with glucose at 2 g $L^{-1}$ concentration. After overnight incubation, to obtain a microbial pellet for inoculation of the testing material, 1 mL culture was centrifuged at 5000 rpm for 5 min; the supernatant was removed and discarded. For testing PDC production, 9.8 mL aliquots of SMB solution were mixed with 200 μL aromatic-containing solvent and inoculated with the microbial pellet. These cultures were incubated for 24 h in an environmental growth chamber at 30 °C with shaking at 200 rpm. After a 24 h incubation period, 1 mL samples were collected and centrifuged at 5000 rpm for 5 min, the supernatant was recovered and filtered, and the samples were stored at −18 °C until further analysis. To determine the growth of *N. aromaticivorans* in the mentioned solution, cell density was assessed with a Klett–Summerson Photoelectric Colorimeter at the time of inoculation and after the 24 h incubation (Fig. S29).

### Analysis of RCF phenolic monomers and PDC

Quantitative analysis of the aromatic monomers was performed on a Shimadzu GCMS-TQ8030 equipped with an AOC-20i autosampler and an Rxi-5Sil MS column (15 m × 0.25 mm × 0.5 μm), with the helium gas mobile phase held at a constant linear velocity of 45 cm $s^{-1}$, and the injection port was set to 250 °C with a split ratio of 20 : 1. The temperature program was as follows: 50 °C for 1 min, then ramped to 300 °C at 20 °C $min^{-1}$, and held at 305 °C for 16.5 min. Calibration curves for the quantified monomers were determined by a ten point calibration curve relative to DMB.[46]

Quantitative analysis of PDC was performed on LC-MS. Quantitative analysis of PDC was accomplished by using a Shimadzu triple-quadrupole liquid chromatography-mass spectrometer. The mobile phase was a binary gradient that consisted of a mixture of water containing 0.1% formic acid and MeOH. The stationary phase was a Kinetex F5 column

(Phenomenex, 2.6 μm pore size, 2.1 mm ID, 150 mm length, P/N: 00F-4723-AN). PDC was detected by multiple-reaction-monitoring (MRM), quantified by use of a standard curve measuring the strongest MRM transition.[11]

### Regression of experimental yields against solubility parameters

We developed a regression model to quantitatively correlate experimentally measured RCF yields with Hansen solubility parameters (HSPs) as descriptors of solvent mixtures. The three HSPs quantify the strength of dispersion interactions ($\delta_D$), dipole–dipole interactions ($\delta_P$), and hydrogen bonding interactions ($\delta_H$). HSPs for a wide range of pure solvents have been tabulated based on empirical measurements,[48] whereas the HSPs for solvent mixtures can be calculated using the volume-fraction-weighted average of individual solvent parameters. HSPs for all pure solvents and their aqueous mixtures used in the RCF experiments are provided in Table S5. We used these three HSPs as descriptors in our regression models for all solvent systems with all values normalized between 0 and 1 for model training purposes based on the maximum and minimum value of each HSP (detailed in the SI).

We performed polynomial regression to correlate descriptors against the experimental RCF monomer yields by using the Automated Learning of Algebraic Models (ALAMO) approach.[59–61] ALAMO automatically evaluates possible algebraic models and is suitable for identifying optimal models for simple regression problems.[61] In our study, we used ALAMO to fit a polynomial regression model that includes parameters corresponding to interaction terms between descriptors (*i.e.*, products of descriptors) as described by the following eqn (4):

$$\begin{aligned}
\text{Yield (wt\%)} = {} & \beta_0 + \beta_1 \delta_D + \beta_2 \delta_P + \beta_3 \delta_H + \beta_4 \delta_D{}^2 \\
& + \beta_5 \delta_P{}^2 + \beta_6 \delta_H{}^2 + \beta_7 (\delta_D \times \delta_P) \\
& + \beta_8 (\delta_P \times \delta_H) + \beta_9 (\delta_D \times \delta_H)
\end{aligned} \quad (4)$$

where $\beta_0$–$\beta_9$ are the regression coefficients. ALAMO selects the best model based on minimizing the corrected Mallow's Cp,[61] which includes eliminating parameters by setting their corresponding coefficients to zero to optimize the tradeoff between model simplicity (*i.e.*, fewer parameters) and accuracy.[62–64] Model accuracy was assessed by computing the root-mean-square-error (RMSE) and $R^2$ for model-predicted yields compared to experimentally determined RCF yields. For comparison with the best model identified from ALAMO, the accuracy of a simple linear regression model was determined by parameterizing the model with the coefficients $\beta_4$–$\beta_9$ set to zero. We also performed leave-one-solvent-out cross-validation to assess the ability of the model to predict yields for previously unseen solvents, as further described in the SI.

### Process synthesis and description

Based on experimental results, an integrated biomass-to-PDC process employing RCF for biomass pretreatment was developed to evaluate the techno-economic performance of twelve

systems: (1) six pure solvents, and (2) 50% v/v solvent/water systems. While we experimentally tested many solvent/water variations, we chose to analyze the 50% v/v mixtures because these systems yielded the highest monomer and PDC production (Fig. 11). We assume an *n*th-plant design with a basis of 2000 dry metric ton per day biomass feedstock rate.

Fig. 12 illustrates the general biorefinery block flow diagram, comprising nine blocks: (1) reductive catalytic fractionation (RCF), (2) monomer purification (MNP), (3) PDC production (PDCP), (4) PDC product isolation (PDCI), (5) hydrolysis of carbohydrate-pulp (HYD), (6) fermentation of sugars to ethanol (FERM), (7) ethanol separation and recovery (SEP), (8) wastewater treatment (WWT), and (9) combined heat and power generation (CHP).

Biomass, solvent, and hydrogen (streams 1–3) are introduced into RCF reactors (2-hour residence time) in the presence of a 5 wt% Pd/C catalyst (assumed to be enclosed in a catalyst basket)[8] in the RCF block for monomer production (see Table S8 for the biomass composition). Solvent and hydrogen from the reactor effluent are recovered and recycled to

reduce fresh input requirements. The reactor effluent is sent to a solid–liquid separation, isolating the carbohydrate-rich pulp from the lignin-derived fraction. The carbohydrate-pulp (stream 4) is routed to the HYD and FERM blocks for enzymatic hydrolysis and fermentation to ethanol, respectively, with ethanol recovered in the SEP block (stream 11), following a process consistent with that used by Humbird *et al.*, 2011.[65] Stream 6 is routed to the MNP block where the monomer is separated. Residual solvent (stream 14) is recycled back to the RCF block, while the monomer (stream 15) is sent downstream to the PDCP block for microbial funneling to PDC, with the oligomer stream (stream 16) sent for heat and power generation. Stream 17 containing nutrient growth media is introduced to support microbial funneling. The resulting fermentation broth containing PDC (stream 18) is then sent to the PDCI block, where PDC is isolated using sodium chloride (stream 19), and recovered as final product (stream 21), while the process wastewater (stream 20) is sent for wastewater treatment. In the solvent/water systems, partial recovery of water is allowed since water is part of the solvent mixture fed to the RCF reactors. The RCF and MNP blocks were modeled and simulated using Aspen Plus (V14). A comprehensive process description and the operating conditions for each system and the key process data are provided in Table S9 and Fig. S12–23.

### Technoeconomic analysis

The economic analysis is performed using the net present value (NPV) approach to calculate the minimum selling price (MSP) of $Na(PDC)_2$ salt required to support the sale of biofuel (ethanol) at $2.50 per gasoline gallon equivalent (GGE). First, the total capital investment, comprising direct and indirect costs, and working capital, is estimated based on equipment costs. Annual fixed operating costs (labor, supervision, overhead) and variable operating costs (biomass feedstock, make-up solvent and hydrogen, catalysts, *etc.*) are then calculated. The MSP, which is the break-even price, is calculated using a discounted cash flow at a fixed after-tax internal rate of return over a 30-year plant lifetime, with NPV set to a value of zero. The economic data and assumptions are provided in Table S10.[10,65–67]
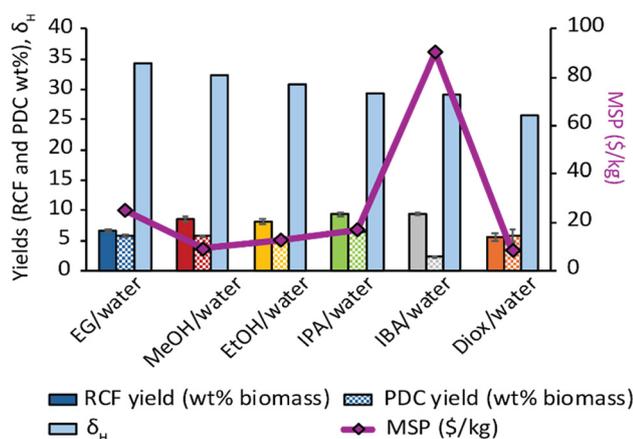


**Fig. 11** Solvent selection for the biomass-to-PDC pipeline based on RCF monomer and PDC yields, operating pressure, $\delta_H$ values, and MSP obtained with aqueous mixtures (50 vol%).
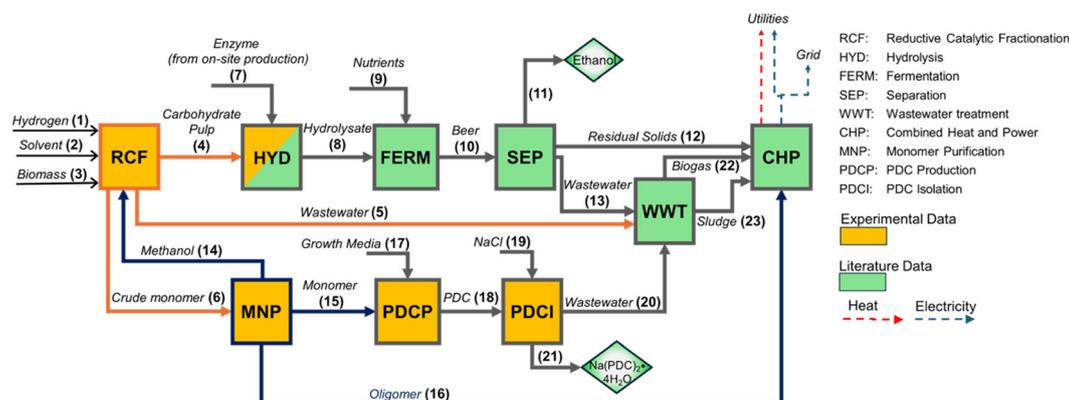


**Fig. 12** Block flow diagram of biorefinery. Stream numbers are in parentheses (adapted and modified from Sener *et al.*, 2026).[30]

### Life cycle analysis

The functional unit for the attributional life cycle analysis (LCA) is 1 kg of Na(PDC)$_2$-salt. The system boundary is the farm-to-product gate entailing biomass (poplar) cultivation, indirect land use changes, transportation, and materials and energy inputs at the biorefinery (see Table S11 for emission factors).[68,69] Biogenic CO$_2$ emission is assumed to be carbon neutral. We consider offset emissions associated with surplus electricity by assuming it displaces U.S. grid electricity. Mass and economic allocation methods are then applied to calculate the life cycle impact of the Na(PDC)$_2$-salt. Specifically, the impacts from the MNP, PDCP, and PDCI blocks are directly allocated to the Na(PDC)$_2$-salt, while that of the HYD, FERM, and SEP blocks are allotted to the biofuel; all other blocks are allocated based on their respective allocation factors detailed in Tables S12–S23 for each system.

## Author contributions

Project lead and administration: C. S.; project conceptualization: C. S., S. K., R. V. L., C. M., D. N., T. D.; performed the investigation: S. S., J. R., E. A., M. G., S. K., C. S.; experiments: S. S., M. G., S. K., C. S.; modelling: J. R., E. A., R. V. L., C. M.; funding acquisitions: T. D., C. S., S. K., D. N., R. V. L., C. M.; visualization: S. S., J. R., E. A., S. K., C. S.; writing – original draft: S. S., J. R., E. A., S. K., C. S.; writing – review & editing: S. S., J. R., E. A., M. G., T. D., D. N., R. V. L., C. M., S. K., C. S.

## Conflicts of interest

There are no conflicts of interest to declare.

## Data availability

The data for this study have been provided in the supplementary information (SI). Supplementary information is available. See DOI: https://doi.org/10.1039/d5gc06557g.

## Acknowledgements

## References

1 T. Renders, G. Van den Bossche, T. Vangeel, K. Van Aelst and B. Sels, Reductive catalytic fractionation: State of the art of the lignin-first biorefinery, *Curr. Opin. Biotechnol.*, 2019, **56**, 193–201, DOI: 10.1016/j.copbio.2018.12.005.

2 P. Sudarsanam, R. Y. Zhong, S. Van den Bosch, S. M. Coman, V. I. Parvulescu and B. F. Sels, Functionalised heterogeneous catalysts for sustainable biomass valorisation, *Chem. Soc. Rev.*, 2018, **47**, 8349–8402, DOI: 10.1039/c8cs00410b.

3 M. Jahangeer, M. U. Rehman, R. Nelofer, M. Nadeem, B. Munir, W. Smulek, T. Jesionowski and S. A. Qamar, Biotransformation of lignocellulosic biomass to value-added bioproducts: insights into bio-saccharification strategies and potential concerns, *Top. Catal.*, 2025, **68**, 929–950, DOI: 10.1007/s11244-024-01941-9.

4 T. I. Korányi, B. Fridrich, A. Pineda and K. Barta, Development of 'lignin-first' approaches for the valorization of lignocellulosic biomass, *Molecules*, 2020, **25**, 2815, DOI: 10.3390/molecules25122815.

5 J. Baruah, B. K. Nath, R. Sharma, S. Kumar, R. C. Deka, D. C. Baruah and E. Kalita, Recent trends in the pretreatment of lignocellulosic biomass for value-added products, *Front. Energy Res.*, 2018, **6**, 141, DOI: 10.3389/fenrg.2018.00141.

6 W. Schutyser, T. Renders, S. Van den Bosch, S.-F. Koelewijn, G. T. Beckham and B. F. Sels, Chemicals from lignin: an interplay of lignocellulose fractionation, depolymerisation, and upgrading, *Chem. Soc. Rev.*, 2018, **47**, 852–908, DOI: 10.1039/c7cs00566k.

7 R. Rinaldi, R. Jastrzebshi, M. T. Clough, J. Ralph, M. Kennema, P. C. A. Bruijnincx and B. M. Weckhuysen, Paving the way for lignin valorisation: Recent advances in bioengineering, biorefining and catalysis, *Angew. Chem., Int. Ed.*, 2016, **55**, 8164–8215, DOI: 10.1002/anie.201510351.

8 M. M. Abu-Omar, K. Barta, G. T. Beckham, J. S. Luterbacher, J. Ralph, R. Rinaldi, Y. Román-Leshkov, J. S. M. Samec, B. F. Sels and F. Wang, Guidelines for performing lignin-first biorefining, *Energy Environ. Sci.*, 2021, **14**, 262–292, DOI: 10.1039/d0ee02870c.

9 L. A. de Souza, P. M. de Souza, G. T. Wurzler, V. T. da Silva, D. A. Azevedo, R. Wojcieszak and F. B. Noronha, Reductive catalytic fractionation of lignocellulosic biomass: unveiling of the reaction mechanism, *ACS Sustainable Chem. Eng.*, 2023, **11**, 67–77, DOI: 10.1021/acssuschemeng.2c03788.

10 A. W. Bartling, M. L. Stone, R. J. Hanes, A. Bhatt, Y. Zhang, M. J. Biddy, R. Davis, J. S. Kruger, N. E. Thornburg, J. S. Luterbacher, R. Rinaldi, J. S. M. Samec, B. F. Sels, Y. Roman-Leshkov and G. T. Beckham, Techno-economic analysis and life cycle assessment of a biorefinery utilizing reductive catalytic fractionation, *Energy Environ. Sci.*, 2021, **14**, 4147–4168, DOI: 10.1039/d1ee01642c.

11 J. M. Perez, C. Sener, S. Misra, G. E. Umana, J. Coplien, D. Haak, Y. Li, C. T. Maravelias, S. D. Karlen, J. Ralph, T. J. Donohue and D. R. Noguera, Integrating lignin depolymerization with microbial funneling processes using agronomically relevant feedstocks, *Green Chem.*, 2022, **24**, 2795–2811, DOI: 10.1039/d1gc03592d.

12 Y. Liao, S. F. Koelewijn, G. Van den Bossche, J. Van Aelst, S. Van den Bosch, T. Renders, K. Navare, T. Nicolai, K. Van Aelst, M. Maesen, H. Matsushima, J. M. Thevelein, K. Van Acker, B. Lagrain, D. Verboekend and B. F. Sels, A sustainable wood biorefinery for low-carbon footprint chemicals production, *Science*, 2020, **367**, 1385–1390, DOI: 10.1126/science.aau1567.

13 M. Tschulkow, T. Compernolle, S. Van den Bosch, J. Van Aelst, I. Storms, M. Van Dael, G. Van den Bossche, B. Sels and S. Van Passel, Integrated techno-economic assessment of a biorefinery process: The high-end valorization of the lignocellulosic fraction in wood streams, *J. Cleaner Prod.*, 2020, **266**, 122022, DOI: 10.1016/j.jclepro.2020.122022, 122021–122011.

14 B. Daelemans, B. Sridharan, P. Jusner, A. Mukherjee, J. Z. Chen, J. K. Kenny, M. Van Dael, K. Vanbroekhoven, P. J. Deuss, M. L. Stone and E. Feghali, From lignin to market: a technical and economic perspective of reductive depolymerization approaches, *Green Chem.*, 2025, **27**, 13160–13178, DOI: 10.1039/d5gc02316e.

15 X. H. Ouyang, X. M. Huang, J. D. Zhu, M. D. Boot and E. J. M. Hensen, Catalytic conversion of lignin in woody biomass into phenolic monomers in methanol/water mixtures without external hydrogen, *ACS Sustainable Chem. Eng.*, 2019, **7**, 13764–13773, DOI: 10.1021/acssuschemeng.9b01497.

16 J. H. Jang, A. R. C. Morais, M. Browning, D. G. Brandner, J. K. Kenny, L. M. Stanley, R. M. Happs, A. S. Kovvali, J. I. Cutler, Y. Roman-Leshkov, J. R. Bielenberg and G. T. Beckham, Feedstock-agnostic reductive catalytic fractionation in alcohol and alcohol-water mixtures, *Green Chem.*, 2023, **25**, 3660–3670, DOI: 10.1039/d2gc04464a.

17 T. Renders, S. Van den Bosch, T. Vangeel, T. Ennaert, S. F. Koelewijn, G. Van den Bossche, C. M. Courtin, W. Schutyser and B. F. Sels, Synergetic Effects of Alcohol/Water Mixing on the Catalytic Reductive Fractionation of Poplar Wood, *ACS Sustainable Chem. Eng.*, 2016, **4**, 6894–6904, DOI: 10.1021/acssuschemeng.6b01844.

18 N. Yan, C. Zhao, P. J. Dyson, C. Wang, L. T. Liu and Y. Kou, Selective degradation of wood lignin over noble-metal catalysts in a two-step process, *ChemSusChem*, 2008, **1**, 626–629, DOI: 10.1002/Cssc.200800080.

19 Z. Sumer and R. C. Van Lehn, Heuristic Computational Model for Predicting Lignin Solubility in Tailored Organic Solvents, *ACS Sustainable Chem. Eng.*, 2023, **11**, 187–198, DOI: 10.1021/acssuschemeng.2c05199.

20 Z. Sumer and R. C. Van Lehn, Data-centric development of lignin structure-solubility relationships in deep eutectic solvents using molecular simulations, *ACS Sustainable Chem. Eng.*, 2022, **10**, 10144–10156, DOI: 10.1021/acssuschemeng.2c01375.

21 E. C. Achinivu, M. Mohan, H. Choudhary, L. Das, K. X. Huang, H. D. Magurudeniya, V. R. Pidatala, A. George, B. A. Simmons and J. M. Gladden, A predictive toolset for the identification of effective lignocellulosic pretreatment solvents: a case study of solvents tailored for lignin extraction, *Green Chem.*, 2021, **23**, 7269–7289, DOI: 10.1039/d1gc01186c.

22 C. M. Hansen and A. Björkman, The ultrastructure of wood from a solubility parameter point of view, *Holzforschung*, 1998, **52**, 335–344, DOI: 10.1515/hfsg.1998.52.4.335.

23 L. P. Novo and A. A. S. Curvelo, Hansen solubility parameters: A tool for solvent selection for organosolv delignification, *Ind. Eng. Chem. Res.*, 2019, **58**, 14520–14527, DOI: 10.1021/acs.iecr.9b00875.

24 Q. Zhang, X. S. Tan, W. Wang, Q. Yu, Q. Wang, C. L. Miao, Y. Guo, X. S. Zhuang and Z. H. Yuan, Screening solvents based on Hansen solubility parameter theory to depolymerize lignocellulosic biomass efficiently under low temperature, *ACS Sustainable Chem. Eng.*, 2019, **7**, 8678–8686, DOI: 10.1021/acssuschemeng.9b00494.

25 A. K. Chew, S. L. Jiang, W. Q. Zhang, V. M. Zavala and R. C. Van Lehn, Fast predictions of liquid-phase acid-catalyzed reaction rates using molecular dynamics simulations and convolutional neural networks, *Chem. Sci.*, 2020, **11**, 12464–12476, DOI: 10.1039/d0sc03261a.

26 J. J. Varghese and S. H. Mushrif, Origins of complex solvent effects on chemical reactivity and computational tools to investigate them: a review, *React. Chem. Eng.*, 2019, **4**, 165–206, DOI: 10.1039/c8re00226f.

27 F. C. Cheng, T. L. Ouyang, J. P. Sun, T. Jiang and J. J. Luo, Using solubility parameter analysis to understand delignification of poplar and rice straw with catalyzed organosolv fractionation processes, *BioResources*, 2019, **14**, 486–499, DOI: 10.15376/biores.14.1.486-499.

28 T. W. Walker, A. K. Chew, H. X. Li, B. Demir, Z. C. Zhang, G. W. Huber, R. C. Van Lehn and J. A. Dumesic, Universal kinetic solvent effects in acid-catalyzed reactions of biomass-derived oxygenates, *Energy Environ. Sci.*, 2018, **11**, 617–628, DOI: 10.1039/c7ee03432f.

29 Z. H. Sun, B. Fridrich, A. de Santi, S. Elangovan and K. Barta, Bright side of lignin depolymerization: Toward new platform chemicals, *Chem. Rev.*, 2018, **118**, 614–678, DOI: 10.1021/acs.chemrev.7b00588.

30 C. Sener, E. A. Aboagye, S. D. Karlen, J. M. Perez, G. E. Umana, Y. Zhang, J. Serate, T. J. Donohue, D. R. Noguera and C. T. Maravelias, Integrating catalytic fractionation and microbial funneling to produce 2-pyrone-4,6-dicarboxylic acid and ethanol, *Green Chem.*, 2026, **28**, 186–198, DOI: 10.1039/D5GC03986J.

31 F. Brienza, D. Cannella, D. Montesdeoca, I. Cybulska and D. P. Debecker, A guide to lignin valorization in biorefineries: traditional, recent, and forthcoming approaches to convert raw lignocellulose into valuable materials and chemicals, *RSC Sustainability*, 2024, **2**, 37–90, DOI: 10.1039/d3su00140g.

32 W. Schutyser, S. Van den Bosch, T. Renders, T. De Boe, S. F. Koelewijn, A. Dewaele, T. Ennaert, O. Verkinderen, B. Goderis, C. M. Courtin and B. F. Sels, Influence of bio-based solvents on the catalytic reductive fractionation of birch wood, *Green Chem.*, 2015, **17**, 5035–5045, DOI: 10.1039/c5gc01442e.

33  Q. Wang, L.-P. Xiao, Q. Xu, H. Zhang, C. Li and R.-C. Sun, Reductive catalytic fractionation of lignocellulose over copper phyllosilicate nanotube catalysts, *Cell Rep. Phys. Sci.*, 2024, **5**, 102055, DOI: 10.1016/j.xcrp.2024.102055.

34  G. G. Facas, D. G. Brandner, J. R. Bussard, Y. Román-Leshkov and G. T. Beckham, Interdependence of solvent and catalyst selection on low pressure hydrogen-free reductive catalytic fractionation, *ACS Sustainable Chem. Eng.*, 2023, **11**, 4517–4522, DOI: 10.1021/acssuschemeng.2c07394.

35  T. Y. Ren, S. P. You, Z. F. Zhang, Y. F. Wang, W. Qi, R. X. Su and Z. M. He, Highly selective reductive catalytic fractionation at atmospheric pressure without hydrogen, *Green Chem.*, 2021, **23**, 1648–1657, DOI: 10.1039/d0gc03314f.

36  M. Jindal, P. Uniyal and B. Thallada, Reductive catalytic fractionation as a novel pretreatment/lignin-first approach for lignocellulosic biomass valorization: A review, *Bioresour. Technol.*, 2023, **385**, 129396, DOI: 10.1016/j.biortech.2023.129396.

37  L. König-Mattern, E. I. S. Medina, A. O. Komarova, S. Linke, L. Rihko-Struckmann, J. S. Luterbacher and K. Sundmacher, Machine learning-supported solvent design for lignin-first biorefineries and lignin upgrading, *Chem. Eng. J.*, 2024, **495**, 153524, DOI: 10.1016/j.cej.2024.153524.

38  Z. Wu, X. Zhao, J. Zhang, X. Li, Y. Zhang and F. Wang, Ethanol/1,4-dioxane/formic acid as synergistic solvents for the conversion of lignin into high-value added phenolic monomers, *Bioresour. Technol.*, 2019, **278**, 187–194, DOI: 10.1016/j.biortech.2019.01.082.

39  F. Heroguel, X. T. Nguyen and J. S. Luterbacher, Catalyst support and solvent effects during lignin depolymerization and hydrodeoxygenation, *ACS Sustainable Chem. Eng.*, 2019, **7**, 16952–16958, DOI: 10.1021/acssuschemeng.9b03843.

40  H. J. Wan, A. Vitter, R. V. Chaudhari and B. Subramaniam, Kinetic investigations of unusual solvent effects during Ru/C catalyzed hydrogenation of model oxygenates, *J. Catal.*, 2014, **309**, 174–184, DOI: 10.1016/j.jcat.2013.09.020.

41  L. Shuai and J. Luterbacher, Organic solvent effects in biomass conversion reactions, *ChemSusChem*, 2016, **9**, 133–155, DOI: 10.1002/cssc.201501148.

42  O. Yu, C. G. Yoo, C. S. Kim and K. H. Kim, Understanding the effects of ethylene glycol-assisted biomass fractionation parameters on lignin characteristics using a full factorial design and computational modeling, *ACS Omega*, 2019, **4**, 16103–16110, DOI: 10.1021/acsomega.9b02298.

43  F. Brienza, K. Van Aelst, F. Devred, D. Magnin, B. F. Sels, P. Gerin, I. Cybulska and D. P. Debecker, Toward a hydrogen-free reductive catalytic fractionation of wheat straw biomass, *ChemSusChem*, 2023, e202300103, DOI: 10.1002/cssc.20230010, 202300101–202300114.

44  A. R. Abouelela, A. Al Ghatta, P. Verdía, M. S. Koo, J. Lemus and J. P. Hallett, Evaluating the role of water as a cosolvent and an antisolvent in [HSO$_4$]-based protic ionic liquid pretreatment, *ACS Sustainable Chem. Eng.*, 2021, **9**, 10524–10536, DOI: 10.1021/acssuschemeng.1c02299.

45  T. Renders, E. Cooreman, S. Van den Bosch, W. Schutyser, S.-F. Koelewijn, T. Vangeel, A. Deneyer, G. Van den Bossche, C. Courtin and B. Sels, Catalytic lignocellulose biorefining in *n*-butanol/water: a one-pot approach toward phenolics, polyols, and cellulose, *Green Chem.*, 2018, **20**, 4607–4619, DOI: 10.1039/C8GC01031E.

46  C. Sener, V. I. Timokhin, J. Hellinger, J. Ralph and S. D. Karlen, Pd/C promotes C–H bond activation and oxidation of *p*-hydroxybenzoate during hydrogenolysis of poplar, *Nat. Commun.*, 2025, **16**, 5259, DOI: 10.1038/s41467-025-60270-x.

47  W. Arts, K. Van Aelst, E. Cooreman, J. Van Aelst, S. Van den Bosch and B. F. Sels, Stepping away from purified solvents in reductive catalytic fractionation: a step forward towards a disruptive wood biorefinery process, *Energy Environ. Sci.*, 2023, **16**, 2518–2539, DOI: 10.1039/D3EE00965C.

48  A. Abbott and C. M. Hansen, Hansen solubility parameters in practice, Hasen-Solubility.com.

49  D. T. Balogh, A. A. S. Curvelo and R. A. M. C. Degroote, Solvent effects on organosolv Lignin from *Pinus-Caribaea-Hondurensis*, *Holzforschung*, 1992, **46**, 343–348, DOI: 10.1515/hfsg.1992.46.4.343.

50  B. Bujanovic, K. Hirth, S. Ralph, R. Reiner, P. Dongre, C. Mickles, S. D. Karlen, C. Baez and C. Clemons, Use of renewable alcohols in autocatalytic production of aspen organosolv lignins, *ACS Omega*, 2024, **9**, 38227–38247, DOI: 10.1021/acsomega.4c05981.

51  X. J. Lu, L. Lagerquist, K. Eränen, J. Hemming, P. Eklund, L. Estel, S. Leveneur and H. Grénman, Reductive catalytic depolymerization of semi-industrial wood-based lignin, *Ind. Eng. Chem. Res.*, 2021, **60**, 16827–16838, DOI: 10.1021/acs.iecr.1c03154.

52  B. Kim, J. M. Perez, S. D. Karlen, J. Coplien, T. J. Donohue and D. R. Noguera, Achieving high productivity of 2-pyrone-4,6-dicarboxylic acid from aqueous aromatic streams with *Novosphingobium aromaticivorans*, *Green Chem.*, 2024, **26**, 7997–8009, DOI: 10.1039/D4GC01975J.

53  F. Bugli, A. Baldelli, S. Thomas, M. Sgarzi, M. Gigli, C. Crestini, F. Cavani and T. Tabanelli, Improved reductive catalytic fractionation of lignocellulosic biomass through the application of a recyclable magnetic catalyst, *ACS Sustainable Chem. Eng.*, 2024, **12**, 16638–16651, DOI: 10.1021/acssuschemeng.4c05299.

54  E. I. Evstigneev, L. V. Bronov and V. M. Nikitin, Use of a polarographic method in the analysis of lignin functional composition. 1. Studies of model compounds, *Khim. Drev.*, 1979, 71–81.

55  S. Y. Qin, S. Omolabake, A. Diaby, J. P. Li, L. D. González, C. M. Holland, V. M. Zavala, S. S. Stahl and R. C. Van Lehn, Identifying green solvent mixtures for bioproduct separation using Bayesian experimental design, *ACS Sustainable Chem. Eng.*, 2024, **12**, 18634–18647, DOI: 10.1021/acssuschemeng.4c07423.

56  T. Michinobu, M. Bito, Y. Yamada, Y. Katayama, K. Noguchi, E. Masai, M. Nakamura, S. Ohara and K. Shigehara, Molecular properties of 2-pyrone-4,6-dicar-

boxylic acid (PDC) as a stable metabolic intermediate of lignin isolated by fractional precipitation with Na⁺ ion, *Bull. Chem. Soc. Jpn.*, 2007, **80**, 2436–2442, DOI: 10.1246/bcsj.80.2436.

57 M. Perez, W. Kontur, M. Alherech, S. D. Karlen, S. Stahl, T. J. Donohue and D. R. Noguera, Funneling aromatic products of chemically depolymerized lignin into 2-pyrone-4–6-dicarboxylic acid with *Novosphingobium aromaticivorans*, *Green Chem.*, 2019, **21**, 1340–1350, DOI: 10.1039/C8GC03504K.

58 G. E. Umana, J. M. Perez, F. Unda, C.-Y. Lin, C. Sener, S. D. Karlen, S. D. Mansfield, A. Eudes, J. Ralph, T. J. Donohue and D. R. Noguera, Biological funneling of phenolics from transgenic plants engineered to express the bacterial 3-dehydroshikimate dehydratase (*qsuB*) gene, Frontiers in Chemical Engineering, *Catal. Eng.*, 2022, **4**, 1036081–1036012, DOI: 10.3389/fceng.2022.1036084, 1036084.

59 A. Cozad, N. V. Sahinidis and D. C. Miller, Learning surrogate models for simulation-based optimization, *AIChE J.*, 2014, **60**, 2211–2227, DOI: 10.1002/aic.14418.

60 A. Cozad, N. V. Sahinidis and D. C. Miller, A combined first-principles and data-driven approach to model building, *Comput. Chem. Eng.*, 2015, **73**, 116–127, DOI: 10.1016/j.compchemeng.2014.11.010.

61 Z. T. Wilson and N. V. Sahinidis, The ALAMO approach to machine learning, *Comput. Chem. Eng.*, 2017, **106**, 785–795, DOI: 10.1016/j.compchemeng.2017.02.010.

62 H. Akaike, New Look at Statistical-Model Identification, *IEEE Trans. Autom. Control*, 1974, **Ac19**, 716–723, DOI: 10.1109/Tac.1974.1100705.

63 S. Konishi and G. Kitagawa, Information criteria and statistical modeling, in *Information Criteria and Statistical Modeling*, 2008, pp. 1–273, DOI: 10.1007/978-0-387-71887-3.

64 C. L. Mallows, Some Comments on Cp, *Technometrics*, 1973, **15**, 661–675, DOI: 10.2307/1267380.

65 D. Humbird, R. Davis, L. Tao, C. Kinchin, D. Hsu, A. Aden, P. Schoen, J. Lukas, B. Olthof, M. Worley, D. Sexton and D. Dudgeon, *Process design and economics for biochemical conversion of lignocellulosic biomass to ethanol: Dilute-acid pretreatment and enzymatic hydrolysis of corn stover Vol. 303*, Report NREL/TP-5100-47764, National Renewable Energy Laboratory (NREL), Golden, CO, USA, 2011, DOI: 10.2172/1013269.

66 R. E. Davis, N. J. Grundl, L. Tao, M. J. Biddy, E. C. Tan, G. T. Beckham, D. Humbird, D. N. Thompson and M. S. Roni, *Process design and economics for the conversion of lignocellulosic biomass to hydrocarbon fuels and coproducts: 2018 Biochemical design case update; Biochemical deconstruction and conversion of biomass to fuels and products via integrated biorefinery pathways*, Report NREL/TP-5100-71949, National Renewable Energy Laboratory (NREL), Golden, CO, USA, 2018, DOI: 10.2172/1483234.

67 R. Davis, L. Tao, C. Scarlata, E. C. D. Tan, J. Ross, J. Lukas and D. Sexton, *Process design and economics for the conversion of lignocellulosic biomass to hydrocarbons: dilute-acid and enzymatic deconstruction of biomass to sugars and catalytic conversion of sugars to hydrocarbons*, Report NREL/TP-5100-62498, National Renewable Energy Laboratory (NREL), Golden, CO, USA, 2015, DOI: 10.2172/1176746.

68 I. Gelfand, S. K. Hamilton, A. N. Kravchenko, R. D. Jackson, K. D. Thelen and G. P. Robertson, Empirical Evidence for the Potential Climate Benefits of Decarbonizing Light Vehicle Transport in the U.S. with Bioenergy from Purpose-Grown Biomass with and without BECCS, *Environ. Sci. Technol.*, 2020, **54**, 2961–2974, DOI: 10.1021/acs.est.9b07019.

69 M. Wang, A. Elgowainy, U. Lee, K. H. Baek, S. Balchandani, P. T. Benavides, A. Burnham, H. Cai, P. Chen, Y. Gan, U. R. Gracida-Alvarez, T. R. Hawkins, T.-Y. Huang, R. K. Iyer, S. Kar, J. C. Kelly, T. Kim, C. P. Kolodziej, K. Lee, X. Liu, Z. Lu, F. H. Masum, M. Morales, C. Ng, L. Ou, T. K. Poddar, S. Reddi, S. Shukla, U. Singh, L. Sun, P. Sun, P. Vyawahare and J. Zhang, *Summary of Expansions and Updates in R&D GREET® 2023*, Report ANL/ESIA-23/10, Argonne National Laboratory, Lemont, IL, USA, 2023, DOI: 10.2172/2278803.